Aus der Abteilung Kardiologie und Pneumologie

(Prof. Dr. med. G. Hasenfuß)

im Zentrum Innere Medizin

der Medizinischen Fakultät der Universität Göttingen

und

aus dem Department of Pharmacology and Cellular and Molecular Physiology

(PI: Prof. B. E. Ehrlich, Ph.D.)

of Yale University School of Medicine, United States of America

---

Functional roles for chromogranin B: the C-terminal domain regulates intracellular calcium kinetics and neuronal signal initiation sites; the N-terminal domain regulates *de novo* secretory vesicle biogenesis; and chromogranin B expression levels are increasing in experimental autoimmune encephalomyelitis

---

INAUGURAL-DISSERTATION

zur Erlangung des Doktorgrades

der Medizinischen Fakultät

der Georg-August-Universität zu Göttingen

vorgelegt von

Stefan Schmidt

aus

Lüneburg

Göttingen 2013

Alle Experimente wurden an der Yale University School of Medicine (USA) im Department of Pharmacology and Cellular and Molecular Physiology unter der Supervision von Prof. Barbara E. Ehrlich durchgeführt. Alle tierexperimentellen Versuche erfolgten in Übereinstimmung mit den Grundsätzen und Rahmenrichtlinien des Yale University's Institutional Animal Care and Use Committee (IACUC).

Dekan: Prof. Dr. rer. nat. H. K. Kroemer

1. Berichterstatter: Prof. Dr. med. G. Hasenfuß

2. Berichterstatter: Prof. Dr. med. A. El-Armouche

Tag der mündlichen Prüfung: 13.01.2014

1. Table of Contents

1. Table of Contents I
2. List of Abbreviations III
3. Abstract 1
4. Introduction and Context
4.1. Inositol 1,4,5 trisphosphate receptors and binding partners 2
4.2. Chromogranins 5
4.3. Calcium microdomains 11
4.4. Role of chromogranin B in neurodegeneration 16
4.5. Secretory vesicle biogenesis mediated by chromogranins 18
5. Materials and Methods
5.1. Antibodies 19
5.2. Plasmids 19
5.3. Cell culture 20
5.4. Transfection 20
5.5. Neuronal differentiation 20
5.6. Western blot analysis 21
5.7. Light microscopy 21
5.8. Immunocytochemistry 21
5.9. Fura-2 AM calcium imaging and data analysis 21
5.10. Fluo-4 AM calcium imaging and data analysis 22
5.11. Experimental autoimmune encephalomyelitis mice 23
5.12. Brain slices 24
5.13. Data analysis and statistical analysis 24
6. Interpretation and causal analysis of published results
6.1. Expression of CGB fragments in NIH3T3 cells 25
6.2. Effects of the expression of CGB and CGB fragments on calcium signaling in NIH3T3 cells 28
6.3. Effects of CGB and the C-terminal CGB fragment on calcium signaling and signal initiation in neuronally differentiated PC12 cells 34
6.4. Effects of CGB and C- and N-terminal CGB fragments on calcium signaling and signal initiation in neuronally differentiated SHSY5Y cells 38
6.5. Effects of the expression of CGB and CGB fragments on secretory granule biogenesis 44

6.6. Regulation of CGB in an autoimmune encephalomyelitis (EAE) mouse model for multiple sclerosis and summarized results 48

7. Reference List 53

8. Publications

8.1. PUBLICATION: The c-terminal domain of chromogranin B regulates intracellular calcium signaling

8.2. PUBLICATION: The role of chromogranin B in an animal model of multiple sclerosis

2. List of Abbreviations

aa	Amino acids
ATP	Adenosine-5'-trisphosphate
AU	Arbitrary units
Ca^{2+}	Calcium
CaM	Calmodulin
C-CGB	C-terminal of CGB (23aa)
C-Def-CGB	C-terminal deficient form of CGB
CGA	Chromogranin A
CGB	Chromogranin B
CSF	Cerebrospinal fluid
C-SP	Scrambled peptide (23 aa of C-CGB in randomized order)
DAG	Diacylglycerol
EAE	Experimental autoimmune encephalomyelitis
ER	Endoplasmic reticulum
$InsP_3$	Inositol 1,4,5 trisphosphate
$InsP_3R$	Inositol 1,4,5 trisphosphate receptor
$InsP_3Rs$	Inositol 1,4,5 trisphosphate receptors
$InsP_3RI$	Inositol 1,4,5 trisphosphate receptor type I
$InsP_3RII$	Inositol 1,4,5 trisphosphate receptor type II
$InsP_3RIII$	Inositol 1,4,5 trisphosphate receptor type III
kd	Dissociation constant
kDa	Kilo Dalton
LTD	Long-term depression
LTP	Long-term potentiation
mAChR	Muscarinic acetylcholine receptor

mAChRs	Muscarinic acetylcholine receptors
M_1AChR	Muscarinic acetylcholine receptor type I
M_2AChR	Muscarinic acetylcholine receptor type II
mGlurR	Metabotropic glutamate receptor
mGlurR$_1$	Metabotropic glutamate receptor type 1
mGlurR$_5$	Metabotropic glutamate receptor type 5
mGlurRs	Metabotropic glutamate receptors
mM	Millimolar
µM	Micromolar
MS	Multiple sclerosis
N-CGB	N-terminal fragment of CGB (20aa)
N-Def-CGB	N-terminal fragment deficient form of CGB
PC12	Rat pheochromocytoma cell line
pH	Potentia Hydrogenii/ pondus Hydrogenii
PKC	Protein kinase C
PLC	Phospholipase C
RyR	Ryanodine receptor
RyRs	Ryanodine receptors
sec	Seconds
SHSY5Y	Human neuroblastoma cell line
SOD1	Superoxide dismutase 1
SR	Sarcoplasmic reticulum

3. Abstract

The versatility of intracellular calcium as a second messenger is evident by its ability to mediate such opposing events as neuronal cell growth and apoptosis. One leading hypothesis is that calcium regulates such divergent signaling pathways through the use of functional calcium microdomains. In this thesis, the architectural organization of calcium microdomains is expanded to include accessory proteins which significantly affect the kinetics of calcium signaling. Chromogranin B (CGB) is a calcium binding protein found in secretory granules and the lumen of the endoplasmic reticulum (ER). CGB buffers calcium, and binds to and amplifies the activity of the inositol 1,4,5 trisphosphate receptor ($InsP_3R$). Previous studies have identified two conserved domains in CGB: an N-terminal domain (N-CGB) and a C-terminal domain (C-CGB). N-CGB binds to the third intraluminal loop of the $InsP_3R$ and presumably inhibits binding of full-length CGB. This displacement of full-length CGB decreases $InsP_3R$-dependent calcium release, thus altering normal calcium signaling patterns. Here, the role of N-CGB in this process is further characterized, and the heretofore unknown role of C-CGB is identified. Expression of either full-length CGB or C-CGB in cells results in a significant increase in calcium transients. In addition, the calcium signal initiation site in neuronally differentiated PC12 and SHSY5Y cells is affected by C-CGB expression, or altered CGB expression patterns. During the course of these studies, we also found that N-CGB is necessary and sufficient to induce vesicle formation during *de novo* secretory vesicle biogenesis. Our results strongly suggest that CGB is a part of the $InsP_3R$ calcium microdomain, which has numerous regulatory roles, and that CGB plays a critical role in modulating $InsP_3R$-dependent calcium signaling. In fact, dysregulation of CGB has been implicated in the literature in many neurological diseases, consistent with our findings concerning the functional effects of CGB on signal initiation and calcium kinetics in neuronally differentiated cells. Thus, we hypothesize that CGB may be a good candidate for modulating the pathophysiological changes associated with certain neurological diseases. In support of this, we found significant CGB upregulation in the affected brain regions of experimental autoimmune encephalitis (EAE) mice, a mouse model for multiple sclerosis. These results suggest a role for functional CGB-$InsP_3R$ calcium microdomains in disease modifying cellular responses.

4. Introduction and Context

4.1 Inositol 1,4,5 trisphosphate receptors and their binding partners

Intracellular calcium is present in all cell types, where it serves as a versatile second messenger with pleiotropic functions. In most neuronal cells, elevations in intracellular calcium levels are mediated by activation of inositol 1,4,5 trisphosphate receptor ($InsP_3R$) by inositol 1,4,5 trisphosphate ($InsP_3$), which leads to calcium release from intracellular calcium stores. The $InsP_3$ pathway begins with activation of phospholipase C (PLC), which mostly occurs via G-protein coupled receptors (GPCRs) or receptor tyrosine kinases, which in turn are activated by various stimuli, including neurotransmitter release, growth factors, light or hormones, *etc*. PLC hydrolyzes a membrane bound phosphoinositide lipid precursor, phosphatidylinositol 4,5-bisphosphate, to $InsP_3$ and diacylglycerol (DAG). $InsP_3$ then diffuses through the cytosol and mediates $InsP_3R$ channel gating; while DAG activates protein kinase C (PKC), leading to downstream phosphorylation of various proteins (Berridge 1993, Foskett et al. 2007).

The $InsP_3$ superfamily of receptors consists of three isoforms ($InsP_3RI$, II and III) which have >65% sequence similarity, but differ markedly in their biophysical and functional properties, including: affinity for $InsP_3$; signaling response magnitude; and modulation by accessory proteins (Bezprozvanny 2005, Hagar and Ehrlich 2000, Miyakawa et al. 1999). In neuronal cells, $InsP_3RI$ is the predominant isoform, and has been previously linked to signal initiation and calcium oscillations of intracellular calcium levels. In contrast, $InsP_3RIII$ has been proposed to serve as a gatekeeper for high magnitude calcium surges, and is mainly located in the soma of neurons (Johenning et al. 2002).

The $InsP_3Rs$ contain six transmembrane spanning domains with four intraluminal loops, and are localized close to intracellular calcium stores, at the ER membrane and nuclear envelope, but also in the Golgi apparatus and secretory vesicles. Structurally, the $InsP_3Rs$ consist of three separate functional domains: 1) a relatively long N-terminal domain, which contains the ligand binding domain and is located in the cytosol; 2) a C-terminal domain which is important for channel formation and channel gating; and 3) a modulatory domain which plays important

roles in channel modulation and coupling (Foskett et al. 2007, Furuichi et al. 1989, Mikoshiba et al. 1994).

Three-dimensional structures of $InsP_3R$ were solved in 2002, revealing two apparent conformations: a windmill-like structure, and a mushroom-like structure. The transition between these two conformations is believed to be mediated by changes in local calcium concentrations (Hamada et al. 2002); while the function of $InsP_3Rs$ can also be modulated by phosphorylation (Vanderheyden et al. 2009). In addition to the above, $InsP_3R$ function can be regulated by association with specific molecules on the cytosolic portion of $InsP_3R$ channel (which contains more than 85% of the total $InsP_3R$ channel mass). Although less common, $InsP_3R$ channel modulation from the intraluminal side has also been reported, and is associated with a stronger response (Choe and Ehrlich 2006, Jiang et al. 2002).

Many proteins have been identified which associate with the N-terminal cytosolic portion of $InsP_3R$ channels: modulating signaling, trafficking, clustering and other $InsP_3R$ functions. For example, plasma membrane-associated proteins such as Rack-I, RhoA-TRPC1, Na/K-ATPase, TRPC3 and Homer have been shown to directly interact with the $InsP_3R$ (Kiselyov et al. 1998, Mehta et al. 2003, Patterson et al. 2004, Tu et al. 1998, Yuan et al. 2005). Homer, associates with several other proteins, including ryanodine receptor type I (RyRI), NMDA receptors and shank, forming $InsP_3R$ signaling microdomains which are sometimes referred to as macro signal complexes (Feng et al. 2002, Tu et al. 1998, Tu et al. 1999, Worley et al. 2007). $InsP_3R$ also mediates interactions with cytoskeletal proteins, such as talin, actin, vinculin, 4.1N, myosin II and ankyrin, resulting in even more complex interaction networks (Bourguignon and Jin 1995, Sugiyama et al. 2000, Walker et al. 2002, Zhang S et al. 2003). Actin and 4.1N appear to be responsible for regulation of lateral diffusion of the $InsP_3RI$ in the ER membrane, and thus may play important roles in spatiotemporal regulation of intracellular calcium signaling (Mikoshiba 2007, Zhang S et al. 2003).

Most known $InsP_3R$ accessory proteins interact with the N-terminal cytosolic portion of the $InsP_3R$ channel, including: IRBIT, bcl-2, CARP, calmodulin, cytochrome c, NCS1, GAPDH, CIB1, Cdc2, DANGER, CaBP1 and many others (Ando et al. 2006, Boehning et al. 2003, Erin and Billingsley 2004, Hirota et al. 2003, Kasri et al. 2004, Malathi et al. 2005, Patel et al. 1997, Patterson et al. 2005, van

Rossum et al. 2006, Schlecker et al. 2006, White et al. 2006). In fact, only a few proteins are known to interact with the $InsP_3R$ luminal side (*i.e.* from the inside of the ER), such as: Chromogranin A and B (CGA/ CGB), ERp44, calnexin and junctuate (Choe et al. 2004, Higo et al. 2005, Joseph et al. 1999, Thrower et al. 2002, Thrower et al. 2003, Treves et al. 2004). However, of all $InsP_3R$ interacting proteins, chromogranin B (CGB) is the most potent co-activator of $InsP_3R$ channels identified to date: addition of CGB to the luminal side of $InsP_3R$ channels incorporated in planar lipid bilayers results in an approximately 10-fold increase in open probability (Thrower et al. 2003). Considering the strict regulation of intracellular calcium concentrations in cells, this $InsP_3R$ channel response may have dramatic consequences, as will be discussed in the following chapters of this thesis.

Physiologically, $InsP_3R$ channels have been shown to play important roles in learning, memory, synaptic plasticity and neurite formation (Rizzuto and Pozzan 2006). Studies using $InsP_3RI$ knockout mice have revealed the importance of $InsP_3R$ channel function for both long-term potentiation (LTP) and long-term depression (LTD), which are models of activity-dependent and long-term structural and functional changes in neurons (Gartner et al. 2006, Miyata et al. 2000, Taufiq et al. 2005, Yoshioka et al. 2010).

4.2 Chromogranins

The granin family consists of 9 proteins, of which chromogranin A (CGA) and chromogranin B (CGB) are the best studied to date. Other members of the granin family include secretogranin II (also referred to as chromogranin C), secretogranins IV-VII, and pro-SAAS. Although first classified as satellite proteins in hormone-storing organelles, granins have since been found in many different tissue types, and their function and overall importance is particularly evident in neurons and secretory cells, such as chromaffin cells (Bartolomucci et al. 2010, Taupenot et al. 2003). Because CGA and, especially, CGB are directly involved in the experiments conducted for this thesis, coverage of other granins in the following sections of this thesis will be minimal.

The CGB gene is located on human chromosome 20, mouse chromosome 2 and rat chromosome 3. The CGB gene product was initially identified in a rat pheochromocytoma cell line (PC12 cells) as a satellite protein in hormone storing organelles. CGB proteins contain between 626 and 657 amino acids (aa), depending on the species or post-translational modifications, with a molecular weight of approximately 76kDa. In addition, CGB contains a disulfide-bonded loop, and can be modified by n- and o-glycosylation, as well as phosphorylation and sulforylation. Chemically, CGB has an unusually high content of acidic amino acids (24%) and proline, with an isoelectric point between 5.1 and 5.2 (Benedum et al. 1987, Helle 2004, Taupenot et al. 2003).

Structurally, five exons in the CGB gene encode five structural domains in the CGB protein. Comparison of CGA with CGB reveals high amino acid sequence similarity in the N- and C-terminal ends of the proteins in humans as well as in other species. The N-terminus of both CGA and CGB is encoded by exon three, while the C-terminus is encoded by exon five in CGB and exon eight in CGA. Overall, both proteins contain only two cysteine residues, which are both located in the homologous N-terminus of CGA and CGB. Sequence identity between CGA and CGB is >54% in the N-terminal region, and >44% in the C-terminal region: most differences are conservative amino acid changes. The two cysteine residues in the N-terminus of CGA and CGB are disulfide bonded, forming a highly conserved 20 aa loop structure. The intervening regions between the N- and C-termini of CGA and

CGB have low sequence similarity, and make up >85% of the protein (Benedum et al. 1987, Helle 2004).

Functionally, CGB has been shown to be a low-affinity, high-capacity calcium binding protein (Gorr et al. 1989), which binds approximately 90 mol of Ca^{2+} per mol, with a dissociation constant (kd) of 1,5 to 3,1 mM (Yoo 2010). It was further shown that CGB induces secretory granule biogenesis – even in non-secretory cells - and that this granulogenic effect is over 50% greater than that of CGA; whereas down-regulation of CGA or CGB results in a markedly reduced number of secretory vesicles in PC12 cells (Huh et al. 2005). Interestingly, CGB has also been found in the nucleus, where it regulates gene transcription, including for genes encoding transcription factors (Yoo et al. 2002). Very recently, insulin secretion in CGB-knock-out mice was examined: although CGB-knock-out mice have more immature insulin granules and a loss of rapid insulin secretion phase, CGB does not seem to be required for the formation of functional insulin granules. However, despite the results from these CGB-knock-out mice studies, the controversy over whether or not chromogranins physiologically induce granule formation remained unsolved (Obermuller et al. 2010).

Chromogranins also play a role in releasing hormones from hormone storing organelles, where they are cleaved into various bioactive peptides upon release into the extracellular space. Several of these CGB-derived peptides inhibit microbial or fungal growth. Although normally they only circulate at low nanomolar concentrations in human blood, the concentrations of some of these CGB-derived peptides can be magnitudes higher in patients with neuronal, neuroendocrine or endocrine tumors. In fact, bloodstream concentrations of some CGB-derived peptides can be reliably used as biomarkers, and are predictive of tumor mass. Once released into the extracellular space, chromogranins are cleaved by endopeptidases, such as the prohormone convertase I and II. However, the degree of processing is highly tissue dependent, and is highest in the nervous system (Gill et al. 1991, Helle 2004, Li et al. 1999, Lovisetti-Scamihorn et al. 1999, Taupenot et al. 2003).

Recently, both CGB and CGA were shown to associate with the luminal side of the $InsP_3R$ in a pH-dependent manner. Specifically, at pH of 5,5 (the pH observed in secretory vesicles) both CGA and CGB associate with the $InsP_3R$; however, when the pH is raised to 7,5 (the pH found in the ER lumen) CGA totally dissociates from

the $InsP_3R$, but CGB only partially dissociates. Interestingly, CGA and CGB spontaneously form CGA/CGB heterodimers at pH 7.5 and CGA_2/CGB_2 heterotetramers at pH 5,5. In planar lipid bilayer experiments, purified $InsP_3RI$ was incorporated into lipid bilayers to measure the effects of chromogranin addition on $InsP_3R$ channel function. At a fixed concentration of $InsP_3$ and calcium on the cis side, the mean channel open time increased from 3,1 ± 0,3 ms to 217,4 ± 0,3 ms and the open probability of the channel increased from 5,0 ± 1,0 % to 80,0 ± 9,0 % upon addition of CGB to the cis side at a pH of 5,5. However, at pH 7,5, the mean open time increased from 4,8 ± 0,6 ms to 122,5 ± 0,7 ms, and the open probability increased from 4,0 ± 1,0 % to 40,0 ± 2,0 %. In addition, the values obtained at pH 7,5 were essentially identical for CGA/CGB heterodimers as for CGB alone (Thrower et al. 2003).

It was later discovered that the interaction between CGB and CGA and the $InsP_3Rs$ is mediated through the N-terminal portion of both chromogranin proteins, which share – as mentioned above – high sequence similarity in this region. Specifically, the N-terminal portions of both CGB and CGA bind to the L3-2 intraluminal loop of the $InsP_3RI$. Moreover, the intraluminal loop L3-2 of the $InsP_3R$ is conserved between the three isoforms of $InsP_3Rs$, suggesting that all three isoforms are capable of binding CGB and CGA (Kang et al. 2007). It was previously believed that the N-terminal portion of CGA or CGB is sufficient to elicit the functional effects of full-length chromogranins on $InsP_3R$ channels; however, expression of the N-terminal portion of CGB in PC12 cells resulted in inhibition of intracellular calcium signaling. These results led to a new hypothesis, that the observed inhibition of calcium signaling is due to the fact that the N-terminal portion of CGB inhibits binding of full-length CGB to the $InsP_3R$, and thus inhibits the activating effects of CGB on the $InsP_3R$ channel. It was further shown that addition of the N-terminal fragment of CGB in planar lipid bilayer experiments markedly reduced $InsP_3R$ channel openings when added to the *trans* side of the bilayer, at fixed concentrations of calcium, $InsP_3$ and CGA/CGB heteromers (Choe et al. 2004).

More recently, expression of the N-terminal fragment of CGB in neuronally differentiated PC12 cells was found to disrupt the interaction between CGB and $InsP_3RI$, resulting in major changes in calcium kinetics and signal initiation sites. However, to fully appreciate the meaning of these elegant experiments, the

distribution of CGB, $InsP_3Rs$ and various other proteins and channels involved in calcium signaling must be taken into account. In neuronally differentiated PC12 cells, CGB is mainly located in growth cones and neuritic branching points. $InsP_3RI$ was found to be homogeneously expressed throughout the cell; whereas staining for the $InsP_3RIII$ was confined to the cytosol and $InsP_3RII$ was not detected. The ER was found to form an extended structure throughout the entire neuron, and no concentration gradient could be detected (Johenning et al. 2002). Calcium ATPases, such as those present in the SR (SERCAII) and plasma membrane (PCMCA1), which extrude calcium from the cytoplasm, were also evenly distributed (Jacob et al. 2005). Because carbachol was used to induce Ca^{2+} release by $InsP_3R$, the distribution of muscarinic acetylcholine receptor (mAChR) - and especially PLC coupled subtypes M_1 and M_2 - was also investigated. Although immunoreactivity of mAChR subtypes M_1 and M_2 could be detected along the neuritic plasma membrane, the majority of clusters were associated with plasma membrane lining the soma. Thus, when stimulated with carbachol, the highest $InsP_3$ concentrations should be generated in the soma, and the calcium signal initiation site should be located there. Surprisingly – depending on the concentration of carbachol – calcium waves were found to begin in 95% of the neurites with a delay of the first somatic signal of 1,7 ± 0,5 sec for 500 µM carbachol, and 3,4 ± 0,6 sec for 50 µM carbachol. After a series of experiments, it was proposed that this temporal delay between the first neuritic and somatic signal could be due to a lowering of the activation threshold in the neurite/growth cone for $InsP_3$ mediated initiation and propagation of calcium signals (Jacob et al. 2005, Johenning et al. 2002).

Although focal gradients of $InsP_3$ could account for the above described phenomenon, most clusters of mAChRs could be detected along the somatic plasma membrane. To further investigate, a mathematical model was constructed using a Virtual Cell Programming Platform, and simulations showed that the concentration of $InsP_3$ inside a neuron should exceed the required threshold within 1 sec. Based on these results, focal gradients of $InsP_3$ cannot explain the observed temporal differences, since this threshold was reached faster than the measured temporal delay between the first neuritic and somatic signal. Consequently, the observed temporal delay must be due to other factors downstream of $InsP_3$ production. Because chromogranins have been shown to enhance the effect on $InsP_3RI$ (under conditions of low $InsP_3$ concentrations) in the above described planer lipid bilayer

experiments, it was assumed that CGB expression in neurites and growth cones could explain the observed effects (Johenning et al. 2002).

To test if the spatiotemporal patterns of Ca^{2+} transients can be effectively predicted by taking into account the accessory proteins that modify $InsP_3R$ function, additional experiments were conducted in PC12 and cultured hippocampal neurons. In cultured hippocampal neurons, the above described ON and OFF mechanisms of calcium signaling were found to be mainly distributed as in PC12 cells, but with a notable difference: CGB staining was only detected in the soma, extending into the proximal dendrite, with no detectable immunostaining in distal neurites. In PC12 cells, the calcium signal was found to initiate in growth cones and neuritic branching points, the compartment of PC12 cells with the highest concentration of CBG. Therefore, if this mechanism really depends on CGB subcellular localization, the calcium signal initiation site in cultured hippocampal neurons should coincide with regions of highest CGB concentrations in the soma and proximal dendrite. Using confocal microscopy and calcium-sensitive flurophores, it was shown that this hypothesis holds true in cultured hippocampal cells: the onset of calcium signaling could be detected in both soma (38% of the time) and proximal dendrites (62% of the time). Furthermore, expression of the N-terminal portion of CGB in neuronally differentiated PC12 cells shifted the calcium signal initiation site from growth cones/neurites to the soma, with a delay of 0,78 ± 0,28 sec. Thus, expression of the N-terminal fragment of CGB appears to not only reverse the calcium signal initiation site from growth cones to the soma, but also markedly decreases the amplitude and flux rate of calcium transients. The mechanism proposed to explain these observed results was disruption of the CGB – $InsP_3R$ interaction by the N-terminal fragment of CGB, which was previously shown to bind to the L3-2 intraluminal loop of the $InsP_3R$ (Jacob et al. 2005).

In summary, CGB was shown to significantly increase the mean open time and open probability of $InsP_3RI$, when added to the *trans* side of planar lipid bilayer experiments *ex vivo* (Thrower et al. 2003). Furthermore, in neuronally differentiated PC12 cells, as well as cultured hippocampal neurons, the calcium signal initiation site was shown to coincide with the subcellular compartment of the cell with the highest concentration of CGB (Jacob et al. 2005). Moreover, CGB was experimentally shown to bind to the L3-2 intraluminal loop of the $InsP_3R$ via the CGB N-terminal region (Kang et al. 2007). In addition, transfection of an interfering polypeptide disrupts this

interaction, resulting in a significantly decreased magnitude of calcium response and flux rate, and a shift (in the case of PC12 cells) of the calcium signal initiation site from growth cones to the soma (Choe et al. 2004, Jacob et al. 2005).

4.3 Calcium microdomains

Because numerous critical processes, such as muscular contractions, cell proliferation and gene transcription are primarily or secondarily calcium-dependent, the concentration of intracellular calcium is closely regulated (Foskett 2010, Mikoshiba 2007). In addition to synergistic events, opposing events, such as apoptosis and neuronal development and growth are mediated by calcium. For quite some time, the spatial organization of calcium channels has been regarded as sufficient to explain even these opposing functions (Berridge 1998). However, this theory has several problems: for example, the mere distribution of calcium channels yields different calcium signaling patterns in different cell types. In addition, although factors modifying $InsP_3R$ response were looked at, neither the concentration of calcium itself nor the concentration of $InsP_3$ can sufficiently explain observed experimental effects.

For example, dendritic spines are only connected to parent dendrites through a very thin neck, and the term “calcium microdomain” has been applied to explain the locally restricted calcium elevations that occur once a spine becomes activated. The architecture of dendritic spines and narrow neck were proposed to enable a local $InsP_3$ gradient to develop and restrict the release of intracellular calcium from ER stacks inside the spine. However, not all dendritic spines are connected to the parent dendrite through a narrow neck. In fact, some spines look like mushrooms, with much wider connecting necks, and stubby spines that are just protuberances of the plasma membrane (Nimchinsky et al. 2002). Moreover, aspiny dendrites were later discovered in neocortical interneurons, fully functional spines which produce highly localized calcium elevations without architectural barriers (Goldberg et al. 2003, Soler-Llavina and Sabatini 2006). In a series of elegant experiments, $InsP_3$ was uncaged in a single dendritic spine, revealing that $InsP_3$ could even diffuse through the very narrow neck of a dendritic spine and activate neighboring spines (Finch and Augustine 1998). Based on these results, the cytosol should be even more effective at producing highly localized calcium surges, with a calcium diffusion rate of 10-50 $\mu M^2/s$ (Allbritton et al. 1992), mediated by calcium binding proteins such as calmodulin, parvalbumin and many others (Schmidt et al. 2003). Experimental data show that less than 1% of the calcium that enters a dendritic spine will diffuse into the dendritic shaft (Sabatini et al. 2002).

Cell type specific interactions between the $InsP_3R$ and accessory proteins might answer questions as to how calcium can accomplish its diverse functions. As mentioned above for neuronally differentiated PC12 cells, CGB and the $InsP_3R$ form a complex where CGB greatly enhances the open probability and mean open time of the $InsP_3R$ channel (Thrower et al. 2003). Because CGB is heterogeneously distributed within the cell, with the highest concentration found in growth cones, CGB is an ideal candidate for explaining how a rise in $InsP_3$ can have different consequences even within the same cell. Additional information on accessory proteins that bind and alter $InsP_3R$ function was given in the previous chapters.

However, interestingly, further research revealed that even more complex interactions might be involved. For example, M_1 muscarinic- (M_1AChR) and B_2 bradykinin- (B_2R) receptors are both G-protein coupled receptors involved in PLC mediated production of $InsP_3$ in non-excitable cells (Felder 1995, Lee and Rhee 1995). However, in excitable neuronal cells, only B_2Rs (and not – or at least to a much lesser extent – M_1AChRs) lead to subsequent $InsP_3R$ mediated calcium release (Bofill-Cardona et al. 2000, Cruzblanca et al. 1998, del Rio et al. 1999). A membrane arrangement that effectively couples B_2R and $InsP_3R$ so that the $InsP_3$ production site is in close contact with the usage site, was proposed to explain these observed effects. Incubation of sympathetic ganglions cells with an inhibitor of actin filament polymerization, followed by addition of the cell-permeant toxin cytochalasin D, disrupted the assumed coupling of B_2R and $InsP_3R$ (Delmas et al. 2002). Such B_2R and $InsP_3R$ coupling has been described previously as an actin bridge, functionally coupling $InsP_3R$ with the plasma membrane in liver cells (Rossier et al. 1991). However, other proteins were identified as well, most notably homer, which tethers mGlurRs with the $InsP_3R$ (Tu et al. 1998).

Long before these experiments were conducted, research has shown that some parts of the ER are in very close contact with the plasma membrane. These regions were called subsurface cisternae, and were further classified into three types, based on their distance from the plasma membrane, which ranges from 20 nm to 80 nm (Berridge 1998).

Based on these results and observations, different, and sometimes conflicting, theories have been proposed to explain the functional relevance of these primary or secondary principles. In fact, to date, no generally accepted theory appears to exist in

the scientific community. Therefore, the following paragraph expresses the author's viewpoint, and citations are used only to underline single observations and results, and do not imply acceptance of the corresponding theory.

If ER-localized $InsP_3Rs$ are also tethered to the plasma membrane through cytoskeletal elements (or whatever elements are involved in the generation of subsurface cisternae), then these complexes basically resemble an architectural barrier, similar to that seen in dendritic spines, which are only connected to the parent dendrite by narrow necks. Although these narrow necks may be of functional importance in some instances, they cannot explain the existence of highly localized calcium elevations. The existence of calcium microdomains consisting of $InsP_3R$ coupled to B_2Rs, or mGluRs, in the plasma membrane does not seem possible if one takes into account results from the following: caged- $InsP_3$ experiments within cells (Finch and Augustine 1998, Miyata et al. 2000); $InsP_3$ diffusion characteristics modeled by a computerized cell programming platform (Johenning et al. 2002); and other experiments and principles mentioned previously in this thesis. Thus, it is the author's own viewpoint that the mere architectural barrier model is not sufficient to explain calcium microdomains, but that they must exist for a reason. Therefore, I believe that we have only scraped the tip of the iceberg with respect to our knowledge of the architectural organization of calcium microdomains. Although single pieces of the puzzle have been discovered, such as actin bridges coupling B_2R and $InsP_3R$ (Rossier et al. 1991) and $InsP_3R$ tethering to mGluRs in the plasma membrane (Tu et al. 1998), we have to perceive these part of a bigger picture, rather than looking at them as single independent principles. Instead of focusing on single events or processes, we have to look how these primary principles are combined. Homer, for instance, is a scaffolding protein that tethers $mGlurR_1$ and $InsP_3R$ in many neuronal cells (Tu et al. 1998). To date, several Homer isoforms have been identified, and all have been shown to bind to the $InsP_3R$ via an N-terminal ENA/VASP homology domain (EVH1). Moreover, a coiled-coil domain in the C-terminal region allows Homer isoforms to oligomerize, forming a meshwork of $InsP_3R$ and $mGlurR_{1,5}$ (Fagni et al. 2002, Kato et al. 1998, Xiao et al. 2000). To add further levels of complexity, the N-terminal domain of Homer also interacts with the PSD-95 complex protein Shank, alpha-adrenergic receptor and TRP channels: Homer can even bind to RyRs via a proline-rich sequence (Feng et al. 2002, Tu et al. 1999, Xiao et al. 2000). In fact, each of these proteins or receptors bind to other scaffolding proteins

and cytoskeletal elements, leading to a meshwork of proteins, receptors, scaffolding proteins and cytoskeletal elements. The result is a mosaic of calcium microdomains that become enmeshed into a calcium microdomain complex, and subsequently, play a role in determining calcium kinetics. Phenomena such as calcium-induced calcium release (CICR) (Berridge 1998) depend on such architectural organizations of calcium channels. In addition, once calcium is released, calcium kinetics can be altered by the nearby receptor organization, via CIRC, or even calcium-induced inhibition of channel activity. Combined, these mechanisms could result in calcium elevations in only a subcompartment of a cell. However, such complex calcium release channel organizations cannot explain the onset, or signal initiation of calcium signals, since they only exert their modulatory effects once calcium release has already been initiated.

Calcium signal initiation is therefore highly likely to depend on the above mentioned accessory proteins, which bind to calcium release channels and modify calcium kinetics. In the previously mentioned experiments involving PC12 and primary hippocampal cells, calcium signals were found to be initiated in the cellular compartment where CGB expression was greatest: in the case of PC12 cells in growth cones, and in the case of primary hippocampal cells in the soma or proximal dendrites (Jacob et al. 2005, Johenning et al. 2002). The impact of RyRs (another ER-localized calcium release channel) on calcium signal initiation is very likely to be of little significance, since RyRs are activated at calcium concentrations over 1 μM, and therefore only begin to modify or magnify local calcium concentrations after initiation by $InsP_3R$ (Bootman et al. 2001). Furthermore, in the model discussed previously, where B_2Rs are linked to $InsP_3Rs$, calmodulin (CaM) was shown to be an important regulator. In fact, CaM has been previously shown to be important for calcium-dependent inactivation of the $InsP_3RI$ (Adkins et al. 2000, Michikawa et al. 1999). In the above mentioned experiments, a CaM mutant with reduced or abolished calcium binding properties was expressed, which contained four point mutations in the EF hand motif. Expression of this CaM mutant changed overall calcium kinetics, resulting in increased peak amplitudes and, more importantly, in a prolonged duration of calcium transients. This effect was attributed to the significantly decreased calcium inactivation rate by the CaM mutant. CaM was proposed by the authors to act as a low-pass filter of $InsP_3$ responses, such that $InsP_3$ production must be fast enough and also great enough to overcome the inhibitory effects of CaM on the $InsP_3R$

channel (Delmas et al. 2002, Delmas and Brown 2002). As a buffer (but not as an amplifier), CaM is unlikely to be a top candidate for regulation of calcium initiation sites; however, in cells where CaM is heterogeneously distributed, CaM-dependent effects might well influence the calcium signal initiation site.

6.4 Role of chromogranin B in neurodegeneration

Neurodegeneration is a term used for the progressive loss of neuronal function, which is attributed to multiple mechanisms, ranging from structural or molecular changes to neuronal cell death. To date, the relationship between CGB and neurodegenerative or neuroinflammatory diseases has only been qualitatively established. However, due to the variety of disease states where CGB is either up- down- or dysregulated, it can be expected that CGB is either directly or indirectly involved in molecular neurodegenerative or neuroimflammatory pathways.

For example, in brain tissues from individuals with Alzheimer's disease, decreased expression of CGB was measured in layers II, III and V of the entorhinal cortex, the inner molecular layers of the dentate gyrus, the CA1 area and the subiculum (Marksteiner et al. 2000). In addition, experimental results from individuals with Parkinson's disease showed increased CGB expression levels in Lewy bodies and axonal swellings. CGB levels in cerebrospinal fluid were likewise significantly increased (Eder et al. 1998, Yasuhara et al. 1994). Moreover, in amyotrophic lateral sclerosis (which leads to fatal degeneration of motor neurons), affected neurons showed superoxide dismutase 1-immunopositive (SOD1) aggregates containing CGA and CGB (Schrott-Fischer et al. 2009). Furthermore, the existence of a CGB mutant variant was identified which affects approximately 10% of all ALS patients (Gros-Louis et al. 2009). CGA and CGB also presumably determine the secretion of mutant SOD1 proteins in individuals with ALS, which are potentially involved in inducing neuronal cell death (Urushitani et al. 2006).

In individuals with schizophrenia, CGB expression was found be to decreased in mossy fibers, hilar interneurons and in CA4 and CA3 regions of the hippocampus (Nowakowski et al. 2002). CGB levels in cerebrospinal fluid were likewise found to be significantly decreased in chronic schizophrenia patients (Landen et al. 1999, Zhang B et al. 2002).

Interestingly, a peptide derived from amino acids 441-493 of CGB was shown to be decreased in the cerebrospinal fluid of patients with multiple sclerosis (MS) (Mattsson et al. 2007). This CGB-derived peptide was previously shown to be decreased in frontotemporal dementia as well (Ruetschi et al. 2005). However, this potential biomarker was not found to correlate significantly with the MS disability

status scale, or any other rating scale or disease characteristics, such as onset age or disease duration (Mattsson et al. 2007).

4.5 Secretory vesicle biogenesis mediated by chromogranins

Two members of the granin family were previously shown to induce secretory vesicle biogenesis: expression of either CGA or CGB in non-secretory cells was shown to be sufficient to induce vesicle formation (Beuret et al. 2004, Huh et al. 2003, Kim et al. 2001). Furthermore, down-regulation of either CGA or CGB in neuroendocrine cells was found to lead to a significant reduction (or even abolishment) of secretory vesicle biogenesis (Huh et al. 2003, Kim et al. 2001). Although both CGA and CGB have been shown to induce vesicle biogenesis, the potency of the two granins in vesicle biogenesis appears to differ: CGB expression is associated with up to 60% more vesicles per cell than CGA expression (Huh et al. 2003). In addition to CGB's very important role in calcium signaling, where it binds between 50-93 mol of Ca^{2+}, in secretory vesicles binding of ATP and catecholamins is also accomplished by CGB (Helle et al. 1990, Phillips 1982, Winkler and Westhead 1980).

Recently, CGA or CGB knock-out mice have become available, and secretory vesicle biogenesis and vesicle sorting in these mice was thus intensively studied. A common observation from these experiments was that when CGA is knocked out, CGB is upregulated in compensation; similarly, when CGB is knocked out, CGA is upregulated (Machado et al. 2010). However, this compensatory mechanism does not appear to be universally valid, since some tissue types do not display significant overexpression of one granin if the other is absent. For example, in pancreatic islets of CGB knock-out mice, compensation of CGA or other members of the granin family was found to occur at a lower extent than in other tissues. Consequently, the lack of CGB in these cells may lead to pathophysiology. Here, for example, the secretion of fewer and more immature granules, coupled with the loss of the initial rapid phase of insulin secretion, is associated with a state of glucose intolerance, similar to the characteristic effects of human type II diabetes mellitus (Obermuller et al. 2010). In these experiments, as well as in experiments conducted with CGA- or CGB knock-out mice by other groups, these *in vitro* results concerning secretory vesicle biogenesis have caused a controversy surrounding the role and importance of CGA and CGB *in vivo*.

5. Materials and Methods

5.1 Antibodies

The following antibodies were used for immunocytochemistry: CGB, BD Biosciences, San Jose, CA, 1:250 or Santa Cruz Biotechnology, Santa Cruz, CA, 1:200; c-myc, Santa Cruz Biotechnology, Santa Cruz, CA, 1:200; calnexin, Stressgen Bioreagents, Ann Arbor, MI, 1:200; $InsP_3R$ type I, affinity purified from rabbit polyclonal antiserum directed against the 19 C-terminal residues of mouse $InsP_3R$ type I, custom made (Research Genetics, Huntsville, AL), 1:300; Alexa Fluor Dyes, Carlsbad, CA, 1:500 to 1:1000.

The following antibodies were used for Western blotting: CGB, QED Biosciences, San Diego, CA, 1:100; anti-rabbit antibodies, Bio-Rad Laboratories, Hercules, CA, 1:50,000. ß-Actin, Abcam, Cambridge, MA, 1:10,000.
The following antibodies were used in the preparation of brain slices: CGB, BD Biosciences, San Jose, CA, 1:250; calnexin, Stressgen Bioreagents, Ann Arbor, MI 1:200; Alexa Fluor Dyes, Carlsbad, CA.

5.2 Plasmids

Murine full-length CGB was kindly provided by Makoto Urushitani (Faculty of Medicine, Laval University, Canada). The N-deficient, and C-deficient fragments of CGB were truncated from full-length CGB. The N-terminal peptide (IIEVLSNALSKSSAPPITPE), C-terminal peptide (ELENLAAMDLELQKIAEKFSQRG), and a scrambled peptide containing the same amino acids as the C-terminal fragment (RLQSALNQDEGEIMALKFLEKAE), were generated by annealing complementary pairs of oligonucleotides corresponding to these peptides (IDT DNA) *in vitro* and cloning them into the pShooter-pCMV/Myc/ER vector (Invitrogen, Carlsbad, CA).

5.3 Cell culture

NIH3T3 cells were grown in DMEM high glucose (4.5g/l) supplemented with 10% fetal bovine serum, penicillin and streptomycin. PC12 cells were grown in DMEM high glucose (4.5g/l) supplemented with 10% heat-inactivated horse serum, 5% heat-inactivated fetal bovine serum, penicillin and streptomycin. SHSY5Y cells were grown in 44% Eagle's minimum essential medium, 44% Ham's F12 medium, 10% fetal bovine serum, 1% non-essential amino acids (100x), penicillin and streptomycin. Cells were cultured in 5% CO_2 at 37°C. All reagents were obtained from Gibco/Invitrogen, Grand Island, NY.

5.4 Transfection

NIH3T3, SHSY5Y and PC12 cells were transfected using Lipofectamine 2000 (Invitrogen, Carlsbad, CA) with full-length, N-deficient, C-deficient, N-terminal, C-terminal, or C-terminal scrambled CGB. To confirm expression, cells were co-transfected with DsRed2 at a ratio of target cDNA to fluorescent protein vector of at least 3:1. NIH3T3 cells were plated in Lab-TeK II 8-well chambers (Nunc/Thermo Fisher Scientific, Rochester, NY); SHSY5Y in 6-well plates (BD Biosciences, Franklin Lakes, NY) on poly-L-lysine coated coverslips (Sigma-Aldrich, St. Louis, MO); and PC12 on collagen I coated coverslips (BD Biosciences, Bedford, MA). Cells were used 48h after transfection.

5.5 Neuronal differentiation

Neuronal cells were differentiated 48h after transfection in antibiotic-free media. Neuronal differentiation of PC12 cells was induced by supplementing growth media with 100 ng/ml nerve growth factor (mNGF 7S, Alomone Laboratories, Israel) for 7 days. SHSY5Y cells were neuronally differentiated by supplementing growth media with 25 ng/ml recombinant human nerve growth factor (ßNGF, Alomone Laboratories, Israel) and 10 µM all-trans retinoic acid (RA) (Sigma-Aldrich, St. Louis, MO) for 8 days. Growth media was changed every other day.

5.6 Western blot analysis

Cells were lysed with M-PER (Thermo Fisher Scientific, Waltham, MA) and centrifuged at 10,000xg at 4°C. Protein concentrations were determined using the BCA Protein Assay Kit (Thermo Fisher Scientific, Waltham, MA). Equal amounts of protein were loaded onto Tris-HCl SDS-PAGE gels (Bio-Rad/Life Science, Hercules, CA) and transferred to PVDF membranes. Membranes were blocked with 5% milk and 0.1% Tween-20 in PBS for 1 hour, followed by incubation with antibodies diluted in blocking buffer. Visualization was performed by chemiluminescence (Amersham, Freiburg, Germany).

5.7 Light microscopy

An Olympus BX60 microscope with a magnification of 100x was used to obtain light microscopy images of transfected NIH3T3 cells with the above described fragments.

5.8 Immunocytochemistry

Cells were fixed in 3.5% paraformaldehyde, permeabilized with 0.1% Triton X, quenched with 0.1 % sodium borohydride in PBS, and blocked in 1% bovine serum albumin and 10% goat serum. Cells were incubated with primary antibody overnight and with secondary antibodies for 1 hour. Coverslips were mounted with ProLong Antifade (Molecular Probes/Invitrogen, Eugene, OR). A confocal 510 LSM microscope (Zeiss, Oberkochen, Germany) was used to visualize the cells.

5.9 Fura-2 AM calcium imaging and data analysis

Transfected NIH3T3 were loaded with 10 μM fura 2-AM (Molecular Probes-Invitrogen, Carlsbad, CA) in a calcium-containing imaging buffer (145mM NaCl/ 5mM KCl/ 2.6mM $MgCl_2$/ 2.6mM $CaCl_2$/ 10mM Hepes/ 5.6 mM glucose, pH 7.4) at 37°C for 30min.

Ratiometric Ca^{2+} imaging in calcium-free imaging buffer containing (145mM NaCl/ 5mM KCl/ 3.6mM $MgCl_2$/ 1mM EGTA/ 10mM Hepes/ 5.6mM glucose, pH 7.4) was performed on a Zeiss Axiovert 100 microscope (Zeiss, Oberkochen, Germany). Intracellular Ca^{2+} concentrations ($[Ca^{2+}]_i$) were derived from background-subtracted F_{340}/F_{380} fluorescent ratios (R) after *in situ* calibration using $[Ca^{2+}]_i$ (nM) = K_d x ß x $(R - R_{min})/(R_{max} - R)$, where K_d is the dissociation constant of fura 2 for Ca^{2+} at 37°C (225 nM), R_{min} and R_{max} were experimentally determined, and ß was the fluorescence ratio of the emission intensity excited by 380 nm for Ca^{2+}-free compared with Ca^{2+}-saturating imaging buffer. Nonviable cells were identified using the sarco(endo)plasmatic calcium ATPase inhibitor thapsigargin (Calbiochem/EMD Biosciences, La Jolla, CA), and were excluded from analysis. The co-transfection marker DsRed2 was visualized before each experiment, and only cells expressing DsRed2 were considered for analysis.

Released Ca^{2+} (peak and total) was calculated by subtracting baseline $Ca^{2+}$of each individual cell and plotted vs. time. Total Ca^{2+} release (area under the curve) was calculated using the program SigmaPlot (Systat Software, San Jose, CA), and resting Ca^{2+} was determined by averaging the baseline Ca^{2+} of each individual cell over a period of at least 40s in Microsoft Excel (Microsoft, Redmond, WA).

5.10 Fluo-4 AM calcium imaging and data analysis

Transfected PC12 or SHSY5Y cells were loaded in calcium-containing imaging buffer (1.25mM $CaCl_2$/ 20mM Hepes/ 4.7mM KCl/ 1.2mM KH_2PO_4/ 1.0mM $MgSO_4$/ 130mM NaCl, pH 7.4) at 37°C with 10 µM fluo-4 AM (Molecular Probes/Invitrogen, Carlsbad, CA) in 20% Pluronic F127 (Sigma-Aldrich, St. Louis, MO) in DMSO for 30 min at 37°C. Cells were incubated for 15 minutes to allow time for de-esterfication in dye-free extracellular solution. The resulting coverslips were mounted at the bottom of an open, custom-made superfusion chamber onto the stage of a Zeiss LSM 510 NLO confocal microscope. Images were acquired at 4Hz for signal initiation experiments and 2 Hz for calcium kinetic experiments. Calcium-free imaging solution containing 20mM Hepes/ 4.7mM KCl/ 1.2mM KH_2PO_4/ 2.3mM $MgSO_4$/ 130mM NaCl/ 1mM EGTA, pH 7.4 at 37°C was used for all experiments and for the dilution of agonists.

For calcium signaling, cells were excited at 488 nm and the appropriate emission filters were used. Increases in [Ca2+]i were expressed as a ratio of the fluorescence intensity of the calcium imaging dye fluo-4 over baseline fluorescence (F/F_0) and were corrected for background fluorescence F_b ($(F-F_b)/(F_0-F_b)$). The self-ratio method (F/F_0) was used because it is independent of factors such as dye concentration, excitation intensity and detector efficiency. However, intracellular calcium concentrations can be underestimated when large changes occur; therefore the magnitude of the calcium signal reported could be underestimated. PC12 and SHSY5Y cells were divided into different regions of interest (ROI) of the same size from the growth cone down to the soma. The onset of the neuritic/growth cone and somatic signal was determined as the time point at which F/F_0 first reached (and remained) at a level 10% above the interval between F_0 and F_{max}. Nonviable cells, defined as cells that failed to respond to the sarco(endo)plasmatic calcium ATPase inhibitor thapsigargin, were excluded from the analysis. Before each experiment, the co-transfection marker DsRed2 was visualized and only cells expressing DsRed2 were taken for analysis.

5.11 Experimental autoimmune encephalomyelitis mice

All animal research was performed in compliance with policies and guidelines of Yale University's Institutional Animal Care and Use Committee (IACUC).

EAE was induced in female C57BL/6 mice (6 week old, Charles River Laboratory, Massachusetts, USA) by subcutaneous injection with 200 µg myelin oligodendrocyte glycoprotein (MOG35–55; MEVGWYRSPFSRVVHLYRNGK, Keck Facility, Yale University, CT), dissolved in an emulsion of 100 µl of complete Freund's adjuvant containing 0.5 mg of heat killed Mycobacterium tuberculosis (Difco Laboratories, Detroit, MI) and 100 µl of phosphate buffered saline (PBS). 200 ng of Pertussis toxin (List Biological Laboratories, Campbell, CA) was dissolved in PBS and injected intraperitoneally on the day of immunization and 48 h later. Scoring of EAE was determined as follows: 0 - no deficit, 1 - tail paralysis; 2 - unilateral hind limb weakness; 3 - incomplete bilateral hind limb paralysis and/or partial forelimb weakness; 4 - complete hind limb paralysis and partial forelimb weakness; 5 - moribund state or death.

5.12 Brain slices

Brains from C57BL/6 mice were collected 15 to 25 days after induction of EAE, postfixed overnight in 4% paraformaldehyde and frozen. Coronary sections were cut at 40 µm (Leica, Nussloch, Germany) and placed in pH 7.4 phosphate buffer (PB). Immunohistochemistry was performed on sections floating in PB at room temperature. Between each procedure, slices were washed 3x in PB for 5–10 min each. Sections were treated with 1% peroxide, permeabilized using 0.3% Triton X-100 and blocked with 5% normal goat serum (Gibco/Invitrogen, Grand Island, NY). Sections were then incubated with antibodies directed against CGB and calnexin for 24 h at 4°C. Following incubation with primary antibodies, sections were incubated with secondary antibodies for 1 h at room temperature, mounted on slides and visualized by a LSM 510 Zeiss confocal microscope.

5.13 Data analysis and statistical analysis

To determine total calcium release, SigmaPlot was used to calculate the area under the curve, and SigmaStat (Systat Software, San Jose, CA) was used for statistical analysis. Western blots were analyzed with Un-Scan-It Gel Software (Silk Scientific, Orem, UT). Raw imaging data were processed using Workbench 5 imaging software (Indec BioSystems, Santa Clara, CA) for fura-2 experiments and LSM Imaging Software (Zeiss, Oberkochen, Germany) for fluo-4 experiments. Statistical analysis was performed using the *t*-test for two group comparisons, or one-way ANOVA (Holm-Sidak method) for multiple group comparisons. One-way ANOVA (Student-Newman-Keuls method) was used for EAE and vesicle biogenesis experiments. Unless otherwise noted, a p value of ≤ 0.05 was considered to be statistically significant.

6. Interpretation and causal analysis of published results

6.1 Expression of CGB fragments in NIH3T3 cells

In order to study the effects of CGB on intracellular calcium signaling, the following CGB fragments were constructed and subcloned into either pcDNA or pShooter mammalian expression vectors: CGB full length (CGB); the conserved N-terminal domain of CGB (20aa) (N-CGB); the conserved C-terminal of CGB (23aa) (C-CGB); an N-terminal deficient form of CGB (N-Def-CGB); a C-terminal deficient form of CGB (C-Def-CGB); and a scrambled peptide containing the 23 amino acids of C-CGB in random order (C-SP) (figure 01A). The resulting CGB constructs were expressed in non-excitable NIH3T3 cells, a mouse fibroblast cell line lacking endogenous expression of CGB. Expression of individual pcDNA-CGB constructs was confirmed by Western blot analysis using an antibody directed against CGB: CGB, N-Def-CGB and C-Def-CGB could be detected after transfection of NIH3T3 cells. An empty pcDNA vector was used as a negative control in Western blots, and samples derived from empty vector transfected cells did not show up on the blot; similarly, no endogenous CGB could be detected from samples derived from NIH3T3 cells alone. ß-actin was used as a gel loading control. The smaller CGB fragments were coupled to a c-myc motif by subcloning into a pShooter expression vector for detection in Western blot experiments. Wild type NIH3T3 cells and cells transfected with empty pShooter vector were used as negative controls (figure 01B). In order to test if deletion of either the N- or C-terminal region of CGB (*i.e.* N-Def-CGB or C-Def-CGB) removes a sorting or retention motif necessary for retaining CGB inside the ER, we used indirect immunofluorescence studies to pinpoint the expression localization of all CGB fragments. For these experiments, calnexin was used as an ER marker protein and overlap of the expressed CGB fragment with calnexin was regarded as a positive signal consistent with expression and retention inside the ER. CGB, N-Def-CGB and C-Def-CGB were visualized using an antibody directed against CGB; whereas the N-CGB, C-CGB and C-SP fragments were visualized using an antibody directed against the c-myc motif. To ensure expression inside the ER for N-CGB, C-CGB and C-SP, these fragments were coupled to KDEL, an ER-retention motif. All constructs showed significant overlap with the ER marker protein, calnexin, consistent with ER retention (figure 01C).

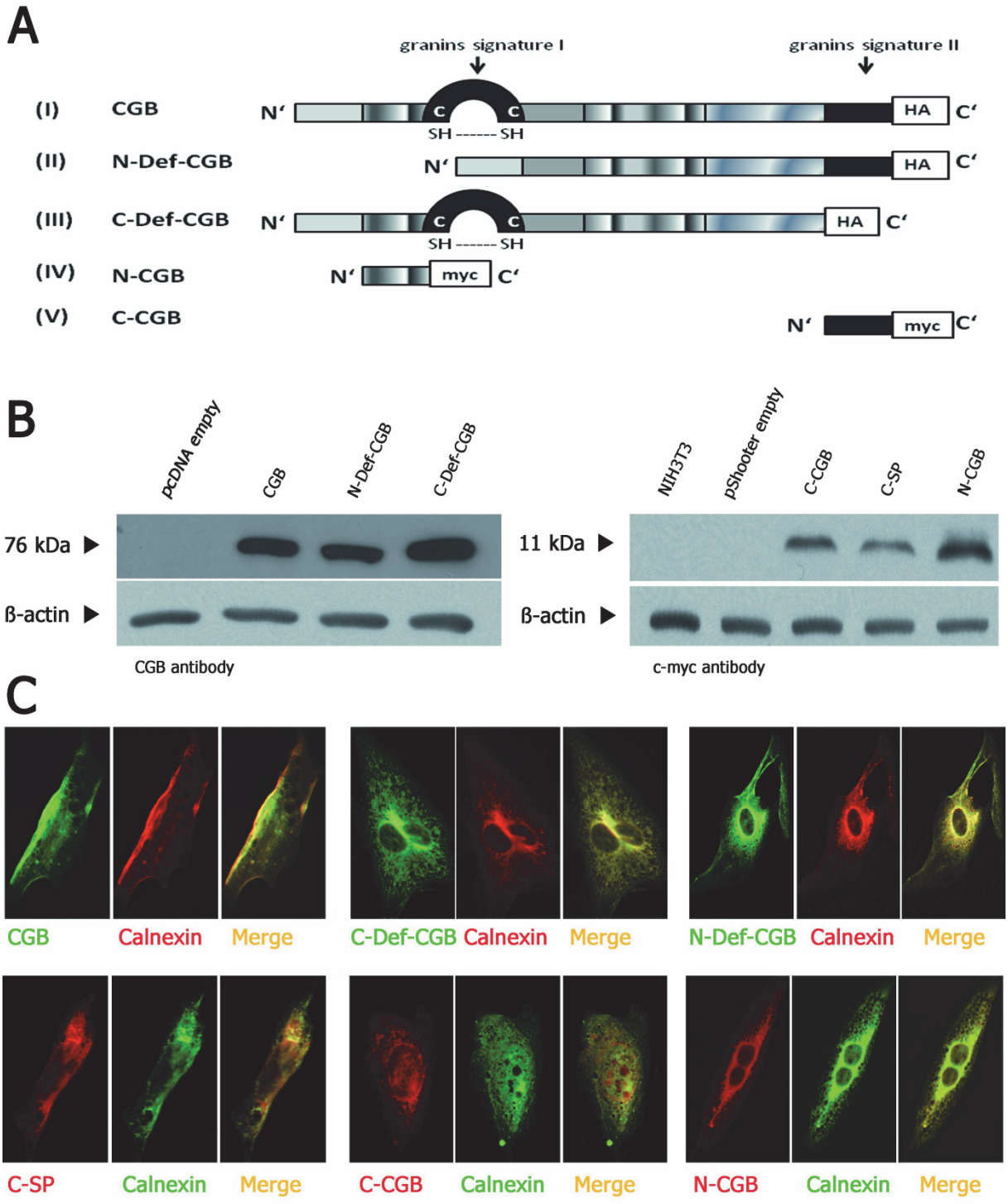

Fig. 01. ***Expression of CGB fragments in NIH3T3 cells.***

(A) *Diagram of CGB constructs: CGB full-length (CGB), the conserved N-terminal of CGB (20aa) (N-CGB), the conserved C-terminal of CGB (23aa) (C-CGB), an N-terminal deficient form of CGB (N-Def-CGB), and a C-terminal deficient form of CGB (C-Def-CGB).* ***(B)*** *CGB fragments were expressed in non-excitable NIH3T3 cells, a mouse fibroblast cell line, and subjected to Western blotting. The empty pcDNA vector and empty pShooter vector were used as negative controls. No endogenous expression of CGB in NIH3T3 cells could be detected. The smaller C-CGB, N-CGB and C-SP fragments were coupled to a c-myc motif*

and visualized with an antibody directed against the c-myc motif. ß-actin was used as a loading control. ***(C)*** *CGB fragments co-localized with the ER-marker protein calnexin, as visualized by immunocytochemistry. Because removal of the N- or C-termini of CGB could have deleted an ER sorting or ER retention motif, immunocytochemistry was used to examine intraluminal ER expression of CGB or CGB fragments, intraluminal ER expression of CGB or CGB fragments was observed, as visualized by overlap with the ER-Protein calnexin. The smaller C-CGB, N-CGB and C-SP fragments were coupled to a KDEL ER-retention motif and intraluminal retention was visualized using an antibody directed against the c-myc motif.*

6.2 Effects of the expression of CGB and CGB fragments on calcium signaling in NIH3T3 cells

Because full-length CGB is itself a potent calcium-binding protein, we initially measured the effects of CGB expression on resting intracellular (cytosolic) calcium levels and ER calcium concentrations in NIH3T3 cells (which lack endogenous CGB). Calcium imaging experiments were conducted on NIH3T3 cells transfected with full-length CGB using the quantitative calcium-sensitive dye fura2-AM: resting intracellular calcium levels were found to be unchanged, with an approximate calcium concentration of 90 nM. The ER calcium concentration in these cells, defined as thapsigargin releasable calcium, was also unchanged, as determined using the sarco(endo)plasmatic reticulum calcium ATPase inhibitor thapsigargin. Similarly, all other CGB fragments had no significant effects on resting calcium levels, or ER calcium concentrations (table 01).

In order to investigate the effects of CGB fragment expression on calcium release, NIH3T3 cells were stimulated using a very low agonist concentration of 1 µM ATP. Under these conditions, peak calcium release was markedly increased by 55%: from 154.4 ± 8.1 nM in the control group to 239.5 ± 33.7 nM in cells transfected with CGB. Peak calcium release in all other treatments groups was not significantly different when compared to the control group. At 1 µM ATP, the duration of calcium elevation over resting levels was increased by 121%: from 27.8 ± 1.5 sec in the control group to 61.5 ± 6.8 sec in cells transfected with CGB. CGB also appears to increase the sensitivity of the $InsP_3R$ to ATP, since the percentage of cells responding to 1µM of agonist concentration increased from 35 to 53% upon CGB expression. In terms of total calcium release, CGB transfected cells were found to release 7.2 times more calcium at very low agonist concentrations, nearly reaching the *in vitro* determined activity rates previously measured in planar lipid bilayers (Thrower et al. 2003). All other CGB fragments failed to induce a significant effect at very low agonist concentrations (figure 02B, table 01).

Interestingly, at medium agonist concentrations (5 µM ATP), both C-CGB and full-length CGB appear to effect intracellular calcium release kinetics. In fact, at 5 µM ATP, C-CGB expression was found to increase peak calcium release by 33%, *versus*

an increase of 28% by full-length CGB: from 299.6 ± 12.7 nM in the control group to 399.7 ± 32.3 nM in the C-CGB group, *vs.* 384 ± 32.3 nM in the CGB group. In addition, although the duration of calcium release was not significantly altered, a trend toward prolonged calcium release was observed for both the CGB and C-CGB groups. In terms of total calcium release, the C-CGB group released 46% more calcium than the control group, while the CGB group released 53% more calcium. All other CGB fragments failed to induce a statistical significant effect at 5μM ATP (figure 02C, table 01). A representative trace and visualized and processed raw calcium imaging data are shown in figure 02A and 03.

When cells were stimulated with high agonist concentration (30μM ATP), peak calcium release levels were not significantly altered, most likely due to saturation of measurable response signals. However, the duration of calcium release was found to be increased in the C-CGB group by 23%: from 77.4 ± 1.6 sec in the control group to 95.3 ± 4 sec in the C-CGB group. Consequently, total calcium release in the C-CGB group increased by 32% vs. the control group (table 01).

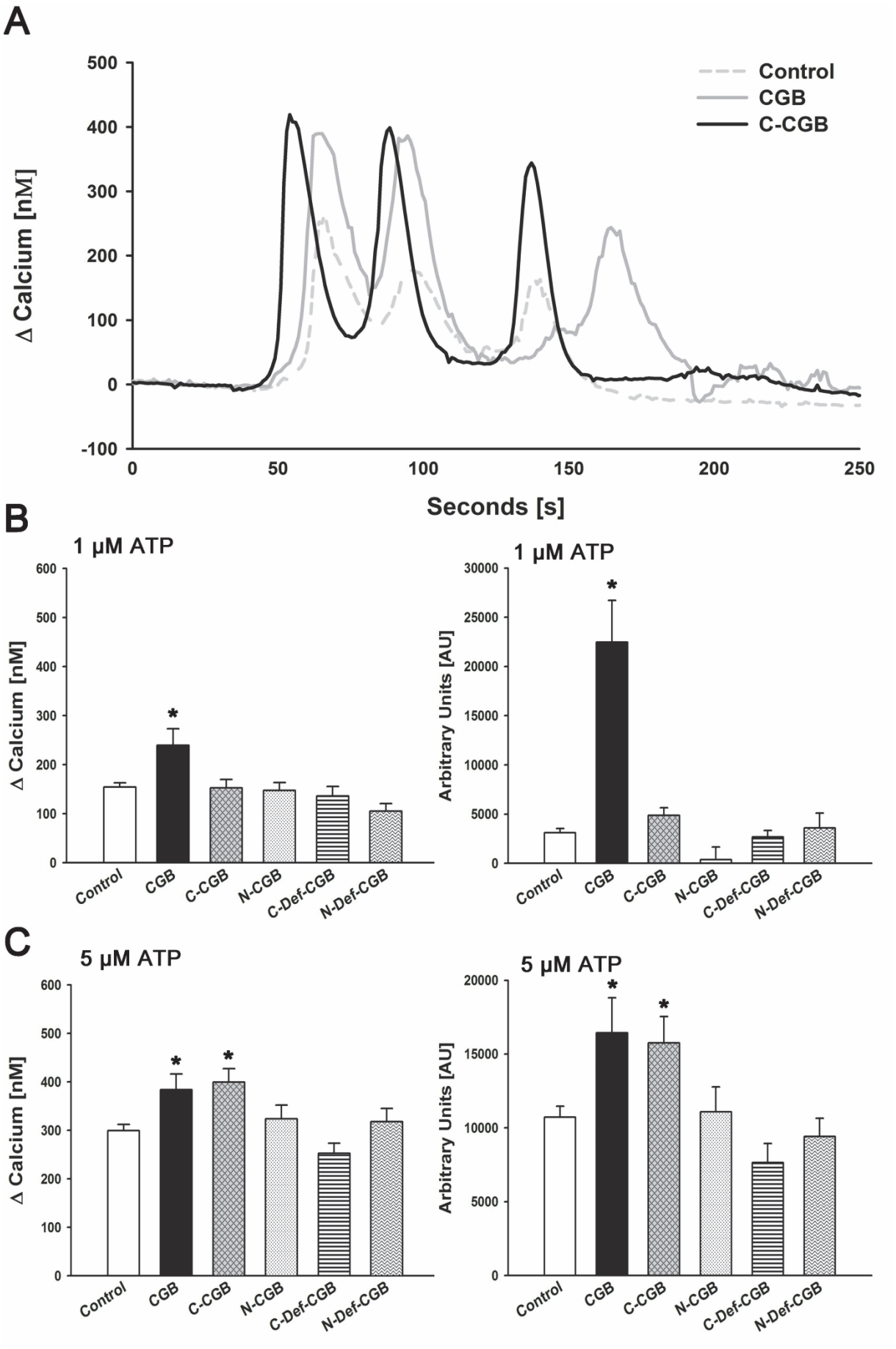
A
Control
CGB
C-CGB
Δ Calcium [nM]
Seconds [s]
B
1 µM ATP
Δ Calcium [nM]
Arbitrary Units [AU]
Control
CGB
C-CGB
N-CGB
C-Def-CGB
N-Def-CGB
C
5 µM ATP

Fig. 02. ***Expression of CGB and C-CGB in NIH3T3 cells increases calcium signal duration, peak calcium release and total calcium release.***

(A) *Representative trace of processed calcium imaging data after stimulation of NIH3T3 cells with 5 µM ATP (corresponding to graphical data in panel C and raw imaging data in Fig. 03). Baseline calcium was subtracted individually from each cell.* ***(B)*** *Peak calcium release in CGB transfected NIH3T3 cells at low agonist concentrations. Stimulation of cells with a very low agonist concentration (1 µM ATP) led to a 55% increase in peak calcium release, from 154.4 ± 8.1 nM in the control group to 239.5 ± 33.7 nM in cells transfected with CGB. CGB transfected cells also released 7.2-fold more total calcium at very low agonist concentrations, nearly reaching in vitro activity rates determined in planar lipid bilayers (Thrower et al. 2003). For additional data see table 01.* ***(C)*** *Peak calcium release in CGB and C-CGB transfected NIH3T3 cells at medium agonist concentrations. At a medium agonist concentration of 5 µM ATP, peak calcium release increased in both CGB and C-CGB expressing cells, from 299.6 ± 12.7 nM in the control group to 399.7 ± 32.3 nM in the C-CGB group and 384 ± 32.3 nM in the CGB group. The C-CGB group released 46% more total calcium and the CGB group released 53% more calcium vs. controls. For additional data see table 01.*

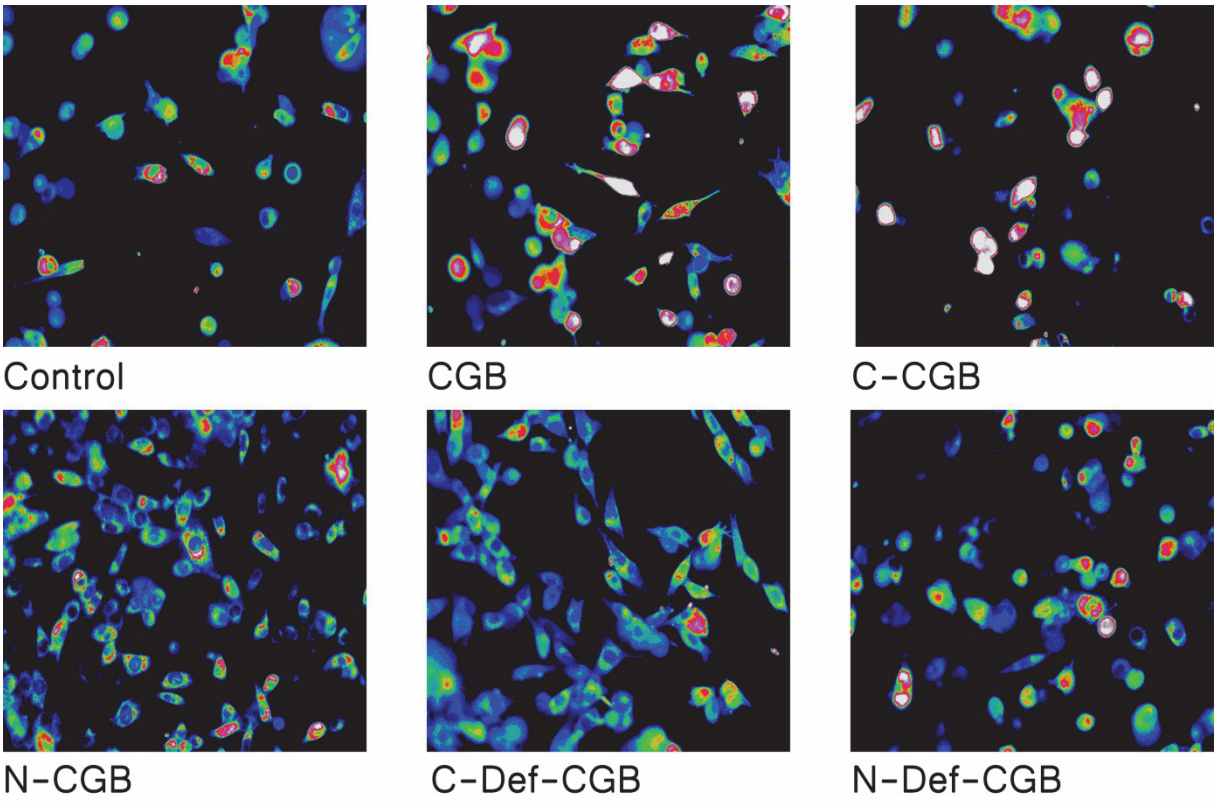

Fig. 03. ***Raw imaging data from ratiometric Fura-2AM calcium imaging experiments.*** *Peak calcium concentrations are shown on a visual scale, ranging from low (coded by the color blue) to high (coded by the color white), after stimulation of NIH3T3 cells with 5 µM*

ATP. Note that to confirm expression, cells were co-transfected with DsRed2 at a ratio of target cDNA to fluorescent protein vector of at least 3:1. Only DsRed2 positive cells were considered for analysis. Thus, not all visible cells have been successfully transfected with the target cDNA.

In summary, at very low agonist concentrations, only full-length CGB was found to be effective at increasing peak calcium release, the duration of calcium release and total calcium release. At medium agonist concentrations (5 μM ATP), both C-CGB and CGB appear to be equally efficient at increasing peak calcium release and total calcium release; whereas at high agonist concentrations (30μM ATP), only C-CGB was efficient at increasing the duration of calcium release and total calcium release (table 01).

Interestingly, the N-terminal CGB (N-CGB) alone failed to have any effect on calcium release kinetics, and NIH3T3 cells do not contain endogenous CGB that could be displaced by N-CGB from the $InsP_3R$ binding site. In addition, N-CGB fragments with truncated C-terminal ends produced calcium kinetics which were similar to the control group. Notably, although the C-terminal region of CGB (C-CGB) had no effect on calcium kinetics at very low agonist concentrations, it was as effective as CGB at medium agonist concentrations, and the only effective CGB fragment at saturating agonist concentration. The lack of effect by C-CGB at low agonist concentrations could possibly be explained by a lowered binding affinity for $InsP_3R$ due to the lack of the N-terminal $InsP_3R$ binding domain. Together, these results strongly support our hypothesis that the C-terminus of CGB contains region(s) which are critical for CGB-mediated effects on calcium kinetics.

	Δ magnitude [nM]			duration [seconds]			response rate [percentage]			total calcium release [AU]			resting calcium [nM]
	1 µM	*5µM*	*30µM*	*1 µM*	*5µM*	*30µM*	*1 µM*	*5µM*	*30µM*	*1 µM*	*5µM*	*30µM*	
Control	154 ± 8	300 ± 13	518 ± 15	28 ± 2	56 ± 2	77 ± 2	35	59	75	3121 ± 416	10735 ± 729	21972 ± 1072	90 ± 1
CGB	**240** ± 34**	**384** ± 32*	507 ± 37	**62** ± 7***	62 ± 5	87 ± 4	54	66	72	**22483** ± 4228***	**16438** ± 2376*	22835 ± 2107	78 ± 2
C-CGB	153 ± 17	**400** ± 27**	533 ± 36	38 ± 4	64 ± 4	**95** ± 4***	32	60	77	4891 ± 762	**15750** ± 1783*	**29128** ± 2611*	88 ± 2
N-CGB	147 ± 16	324 ± 28	512 ± 43	34 ± 5	53 ± 4	75 ± 4	39	64	72	383 ± 1281	11086 ± 1693	19189 ± 1867	119 ± 3
C-def-CGB	136 ± 19	253 ± 21	527 ± 30	30 ± 6	54 ± 5	88 ± 4	24	49	81	2693 ± 643	7654 ± 1290	23920 ± 1707	93 ± 2
N-def-CGB	105 ± 16	318 ± 27	455 ± 40	35 ± 8	57 ± 4	80 ± 6	20	63	77	3588 ± 1530	9422 ± 1235	18979 ± 1918	81 ± 2

Table 01. ***Effects of CGB and CGB fragment expression in NIH3T3 cells.***

*NIH3T3 cells with no endogenous expression of CGB were transfected with CGB fragments as described in the Materials and Methods section (or see figure 01A). 48 hours after transfection, cells were loaded with a fura-2AM calcium imaging dye and live cell ratiometric calcium imaging was performed. Cells were then stimulated with either 1µM, 5µM or 30µM ATP, to induce $InsP_3$ mediated calcium release by $InsP_3Rs$. Peak calcium release, duration of the calcium response, response rate, total calcium release and resting calcium levels are shown in the corresponding columns. Stated values are results from at least 5 different and independent experiments per treatment group. Statistically significant p values are shown in bold and stated as follows: * ≤ 0.01, ** ≤ 0.001, *** ≤ 0.0001.*

6.3 Effects of CGB and the C-terminal CGB fragment on calcium signaling and signal initiation in neuronally differentiated PC12 cells

Previous experiments have shown that CGB is predominantly localized to growth cones and neuritic branching points in neuronally differentiated PC12 cells (Jacob et al. 2005). In these experiments, the calcium signal initiation site coincided with the growth cone, the area with the highest concentration of CGB (Johenning et al. 2002). Moreover, the interaction of CGB with the $InsP_3R$ in the growth cone could be disrupted by expressing a fragment from the N-terminal binding domain of CGB, leading to a shift of the calcium signal initiation site to the soma (Choe et al. 2004, Jacob et al. 2005). The following experiments were designed to confirm whether the calcium signal initiation site always coincides with the area of highest CGB expression, and to test the measured effects of CGB and C-CGB in non-excitable NIH3T3 cells in a cell model of excitable and neuronally differentiated PC12 cells. Previous experiments used carbachol as an agonist. However, in the present study, we used bradykinin as an agonist, since one of our aims was to determine if the calcium microdomain consisting of CGB and $InsP_3RI$ is agonist-independent, and if the effects of CGB on $InsP_3RI$-mediated calcium kinetics are similar regardless of primary stimulus.

Overexpression of CGB in neuronally differentiated PC12 cells that contain endogenous CGB significantly altered the CGB distribution pattern. As expected, in untransfected, neuronally differentiated PC12 cells, we detected the highest amounts of CGB expression in growth cones and neuritic branching points; while CGB expression levels in the soma were minimal. However, interestingly, overexpression of CGB altered this pattern, such that CGB expression levels were distributed between the growth cone and the soma, with a trend toward higher CGB expression in the soma. In fact, taking absolute CGB expression levels into account, most of the expressed CGB was now located in the soma. In contrast, expression of C-CGB in neuronally differentiated PC12 cells resulted in a more even expression distribution between the growth cone and the soma (figure 04-A).

Stimulation of untransfected neuronally differentiated PC12 cells, or cells transfected with scrambled CGB peptide (C-SP), with 2 µM bradykinin resulted in an initial calcium signal at the growth cone, followed by a calcium signal response in the soma (after a 2.26 ± 0.43 sec delay). The measured delay was consistent with previously published values obtained using carbachol instead of bradykinin as an extracellular agonist. Interestingly, in CGB overexpressing cells, which contain the highest concentration of CBG in the soma, the calcium signal initiated first in the soma, followed after a delay of 1.24 ± 0.85 seconds by a response in the growth cone. In C-CGB expressing cells, the neuritic and somatic calcium initiation signals were detected simultaneously (± 0.99 sec) (figure 04-B, table 02).

Peak calcium release was significantly increased in both full-length CGB and C-CGB transfected PC12 cells, with a 6-fold increase in peak calcium release in the CGB overexpressing group, and a 5-fold increase in the C-CGB group (figure 04-B, table 02).

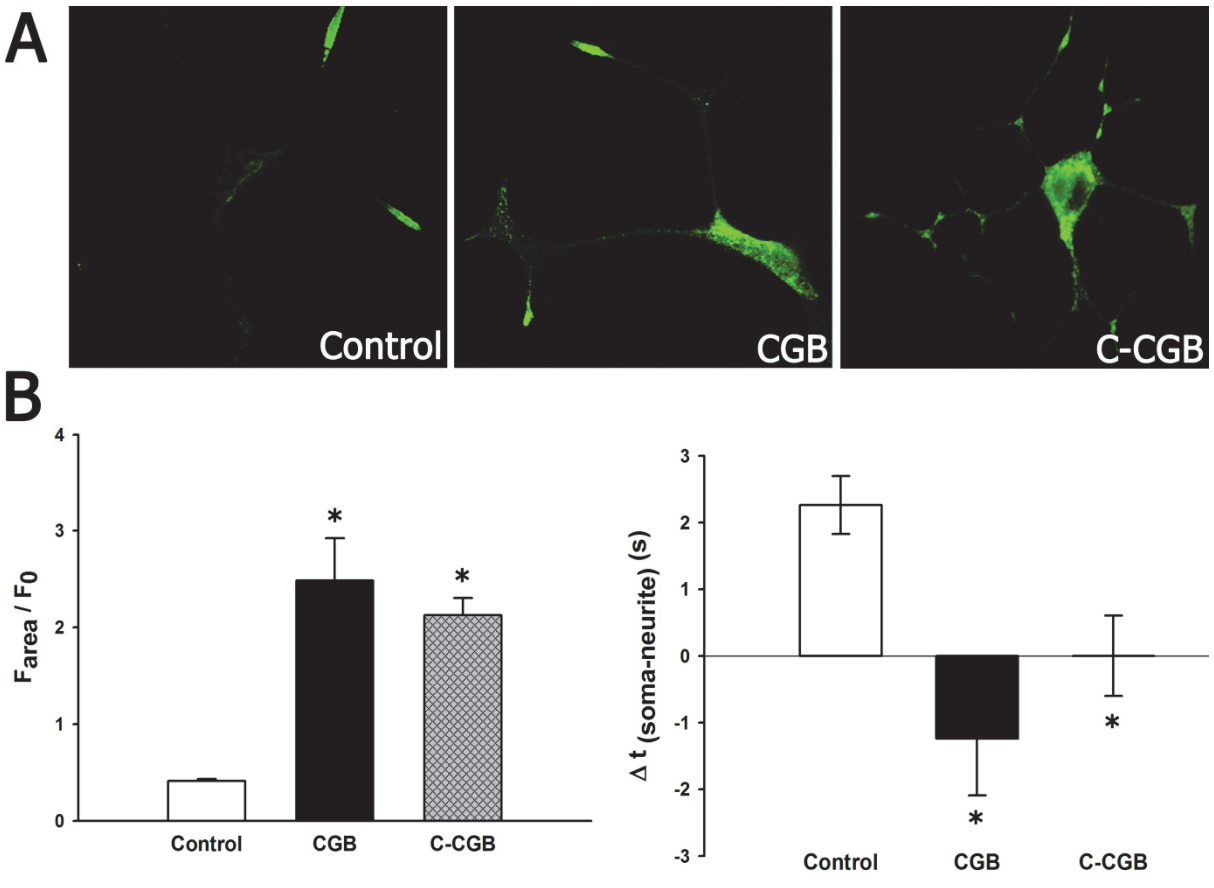

Fig. 04. ***The magnitude of calcium release is increased and calcium signal initiation sites are altered upon expression of C-CGB, or overexpression of CGB, in neuronally differentiated PC12 cells.***

(A) *In untransfected neuronally differentiated PC12 cells, endogenous CGB expression is localized to growth cones and neuritic branch points; whereas expression levels in the soma are minimal. Overexpression of CGB resulted in CGB expression throughout the cell. After taking absolute CGB expression levels into account, most of the expressed CGB appears to be located in the soma. Expression of C-CGB led to more evenly distributed CGB expression levels between growth cones and the soma.* ***(B)*** *Left panel: Peak calcium release was significantly increased upon expression of either C-CGB fragments (5-fold) or overexpression of CGB (6-fold). For additional data see table 02. Right panel: Bradykinin stimulation of neuronally differentiated PC12 cells transfected with scrambled C-CGB (as a control) resulted in calcium signal initiation first appearing in growth cones, followed by a response in the soma after a delay of 2.26 ± 0.43 seconds. In CGB overexpressing cells, with the highest amount of CBG in the soma, the calcium signal first initiated in the soma, followed by a response in the growth cone after a delay of 1.24 ± 0.85 seconds. In C-CGB expressing cells, the first neuritic and somatic signals were detected simultaneously, ± 0.99 sec. For additional data see table 02.*

The above described results represent further evidence that a calcium microdomain consisting of $InsP_3R$ and CGB (or C-CGB) defines the calcium signal initiation site, and that neuronal calcium kinetics, and therefore all calcium-dependent neuronal cell functions, can be modified by alterations in the distribution and/or expression levels of CGB or C-CGB (an endopeptidase cleavage product of full-length CGB). Furthermore, we demonstrated that this $InsP_3R$-CGB calcium microdomain is not agonist specific. In fact, because both rapid (mAChR stimulation with carbachol) and slow (B_2R stimulation with bradykinin) $InsP_3$ production produce similar results, the identical latency time recorded from the first neuritic calcium signal to the first somatic signal must rely on mechanisms downstream of $InsP_3$ production. This assertion is supported by both a previously published virtual cell mathematical model (see section 4.2) and published results from other experiments in neuronally differentiated PC12 cells using caged-$InsP_3$ (see section 4.3) (Johenning et al. 2002). Furthermore, the present results strongly suggest that this function of full-length CGB in neuronally differentiated PC12 cells depends only on the 23 amino acid long C-terminal fragment of CGB (C-CGB).

	Δ magnitude [AU]	**signal initiation [seconds]**
	2 µM	$^{\Delta t}$ *[soma-neurite]* $^{(s)}$
Control	0.41 ± 0.01	2.26 ± 0.43
CGB	**2.48** ± 0.43 ***	**1.24** ± 0.85 **
C-CGB	**2.12** ± 0.17 **	**0.0014** ± 0.60 *

Table 02. ***Effects of C-CGB expression and CGB overexpression in neuronally differentiated PC12 cells.***

*PC12 cells were transfected with the CGB fragments described in the Materials and Methods section (or see figure 01A), and neuronally differentiated for at least 7 days. Neuronal differentiation was induced by incubating the cells in nerve growth factor. Calcium imaging experiments were conducted on a Zeiss NLO confocal microscope, by loading the cells with a calcium-sensitive imaging dye, fluo-4 AM. Expression of CGB or CGB-fragments was confirmed by co-transfecting cells with at least 3-fold lower amount of fluorescent DsRed2 protein. Cells were stimulated with 2 µM of the B_2R agonist bradykinin, and signal initiation sites and calcium kinetics were monitored. Results for peak calcium release and signal initiation sites are shown in the corresponding columns. Stated values are the result of at least 4 different and independent experiments per treatment group. Statistically significant values are shown in bold and stated as follows: * ≤ 0.05, ** ≤ 0.01, *** ≤ 0.001.*

6.4 Effects of CGB and C- and N-terminal CGB fragments on calcium signaling and signal initiation in neuronally differentiated SHSY5Y cells

Neuronally differentiated PC12 cells are a peripheral ganglion cell line, which was originally isolated from a rat pheochromocytoma. PC12 cells are a well-respected and frequently-used model for studying neuronal processes in non-primary cells, because their excitability and signal transduction properties are similar to primary neurons (Appell and Barefoot 1989, Greene and Tischler 1976, Koizumi et al. 1999, Shafer and Atchison 1991). However, PC12 cells also have certain limitations: in some cases, results obtained in PC12 cells cannot be replicated in primary neuronal cells, or using extremely difficult to obtain primary human neuronal cells. Therefore, in an attempt to support and extend our findings, we performed additional experiments using human SHSY5Y neuroblastoma cells. To enable more direct comparison, SHSY5Y cells were neuronally differentiated using retinoic acid and recombinant human nerve growth factor. Successful neuronal differentiation was confirmed by observation of morphological extensions or neuritis, as well as upregulation of CGB expression, which has been shown to increase with neuronal activity. In the present study, CGB expression in neuronally differentiated SHSY5Y cells was indeed upregulated 8-fold vs. controls during the differentiation process, as confirmed by Western blotting (figure 5A + figure 5B + figure 5E).

As a prerequisite for the above described SHSY5Y experiments, we confirmed that InsP3RI, the predominant calcium release channel in neuronal cells, is in fact equally distributed throughout the cell and its extensions. Thus, any possible observed shift in calcium signal initiation site cannot be explained by “hotspots” of InsP3R channels. No significant differences were observed for resting calcium levels in neuronally differentiated SHSY5Y cells expressing CGB or the various CGB fragments. In addition, no changes in the level of ER calcium stores were found, both in terms of peak and total calcium release, as measured using the sarco(endo)plasmic reticulum calcium ATPase inhibitor, thapsigargin (figure 5C + figure 5D).

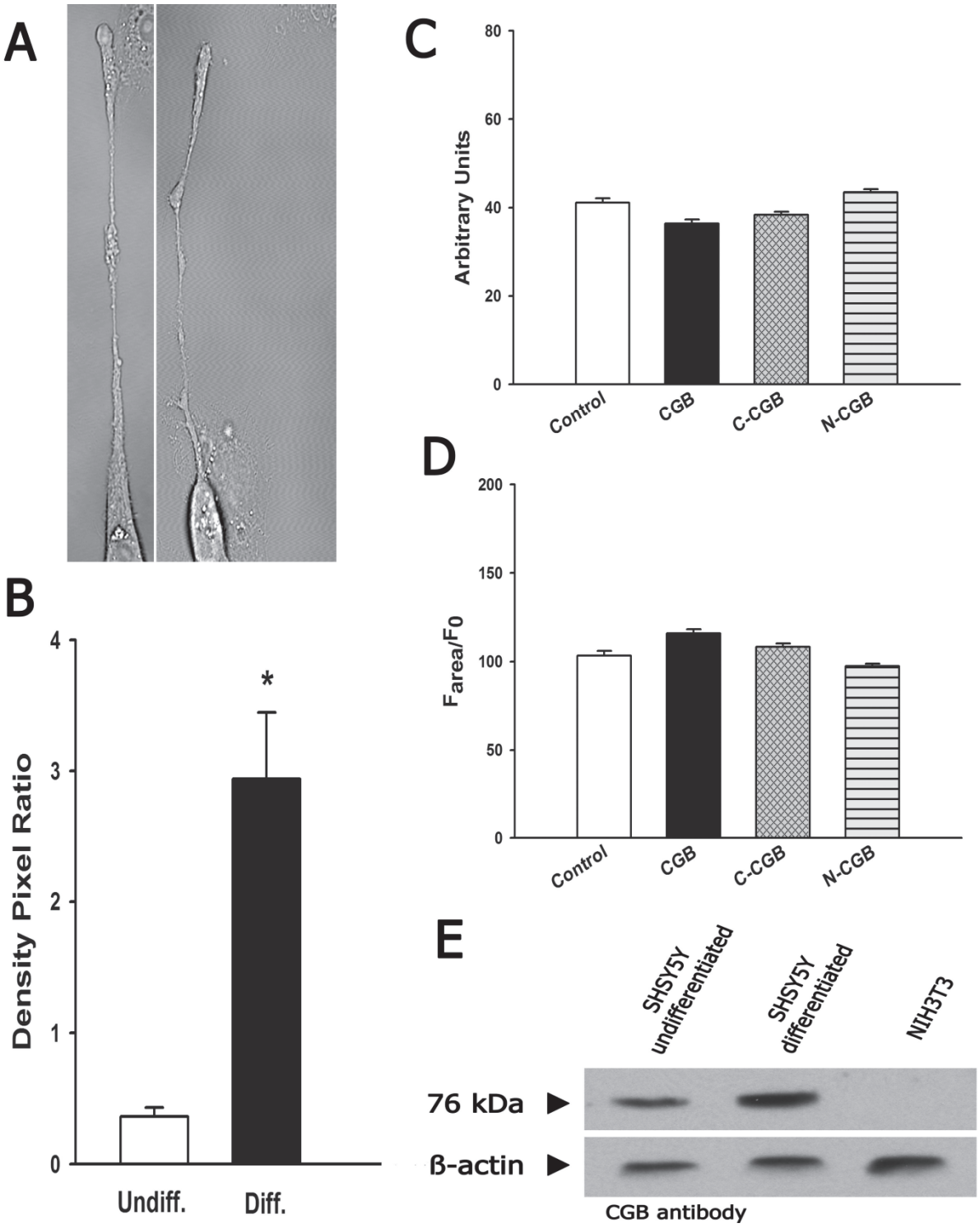

Fig. 05. ***Neuronally differentiated SHSY5Y cells have elevated CGB levels, but expression of CGB or CGB fragments does not alter resting calcium levels.***

(A),(B) *Neuronal differentiation of a human neuroblastoma cell line (SHSY5Y cells) by retinoic acid and recombinant human nerve growth factor was successful as indicated by the development of neurite extensions (A) and Western blotting showing increased CGB levels upon neuronal differentiation (B).* ***(C), (D)*** *Expression of CGB fragments or overexpression of CGB in neuronally differentiated SHSY5Y cells does not change resting calcium levels (C),*

or alter ER calcium levels, defined as thapsigargin-releasable calcium (D). ***(E)*** *Western blot showing increased CGB levels after treatment with retinoic acid and recombinant human nerve growth factor to induce neuronal differentiation.*

In neuronally differentiated SHSY5Y cells stimulated with 15µM of carbachol (an mAChR agonist), the peak calcium response was found to be 93% higher in CGB-expressing cells, and 98% higher in C-CGB expressing cells *versus* the control group. Peak calcium concentrations nearly doubled, increasing from 0.9 ± 0.09 AU for control cells to 1.8 ± 0.1 AU for CGB and 1.8 ± 0.1 AU for C-CGB cells. Consistent with our results from PC12 cells, N-CGB expression was associated with a decrease in peak calcium release of approximately 47%, corresponding to a peak calcium release of only 0.4 ± 0.05 AU (figure 6B, table 03). C-CGB expressing neuronally differentiated SHSY5Y cells responded 68% longer than control cells, corresponding to an increase in calcium signal response time from 99.24 ± 7.53 sec in the control group to 167.01 ± 12.1 seconds in cells expressing C-CGB (figure 6C, table 02). In addition, $InsP_3RI$ sensitivity increased from 59% responding cells in the control group to 80% responding cells in the CGB expressing group; while in the case of C-CGB expression, $InsP_3RI$ sensitivity was measured to be as high as 86% responding cells. In contrast, N-CGB expression actually resulted in an 8% decrease in responding cells (table 03).

Under the conditions used in our experiments, growth cones in the neuronally differentiated SHSY5Y cells appeared to be significantly more sensitive to $InsP_3$-mediated calcium release than the soma. Accordingly, the first calcium signal in SHSY5Y growth cones was detectable 17.18 ± 5.33 seconds before the first somatic calcium signal was observed. Interestingly, CGB expression decreased this delay to 2.62 ± 2.22 seconds. In addition, C-CGB expression resulted in a shift of the calcium initiation site: the first somatic signal was detected 1 ± 2.16 seconds before the first neuritic signal (figure 6C, table 03). Statistically interpreted the somatic and neuritic signals occurred at the same time with a trend towards occurring first in the soma.

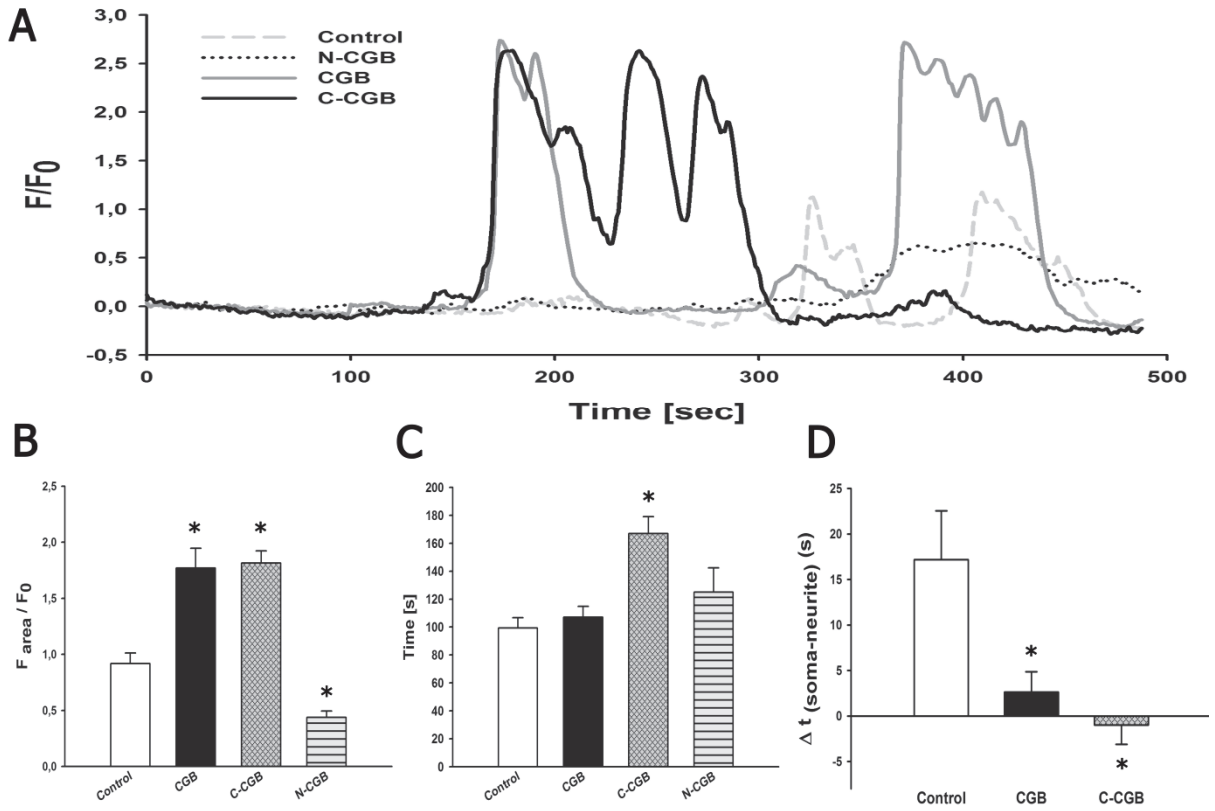

Fig. 06. ***Expression of C-CGB in neuronally differentiated SHSY5Y cells alters the calcium signal initiation site, and is associated with increased peak calcium release and signal duration.***

(A) *Representative trace of processed calcium imaging data. Neuronally differentiated SHSY5Y cells transfected with the different CGB fragments were stimulated with 15µM carbachol. Baseline calcium was subtracted from each cell individually.* ***(A), (B)*** *Peak calcium responses in CGB and C-CGB expressing neuronally differentiated SHSY5Y cells. Peak calcium response was 93% higher in CGB expressing cells, and 98% higher in C-CGB expressing cells versus the control group. Peak calcium concentrations nearly doubled, increasing from 0.9 ± 0.09 AU for control cells to 1.8 ± 0.1 AU for CGB and 1.8 ± 0.1 AU for C-CGB. N-CGB expression led to a 47% decrease in released peak calcium, corresponding to a peak calcium release of only 0.4 ± 0.05 AU.* ***(C)*** *Calcium signal durations in C-CGB expressing cells versus controls. C-CGB cells respond 68% longer than control cells, corresponding to an increase in calcium signal duration from 99.24 ± 7.53 sec in the control group to 167.01 ± 12.1 sec in cells expressing C-CGB.* ***(D)*** *Calcium signal initiation site analysis. An initial calcium signal was detected in the growth cones of SHSY5Y cells 17.18 ± 5.33 sec before the first somatic response was observed. CGB expression decreased this delay to 2.62 ± 2.22 sec. Also, C-CGB expression resulted in a shift of the calcium initiation site: the first somatic signal was now detectable 1 ± 2.16 sec before the first neuritic signal. For additional data see table 03.*

In the above described experiments on neuronally differentiated SHSY5Y cells, we acquired further information about how our proposed calcium microdomain consisting of $InsP_3RI$ and CGB, C-CGB or N-CGB, could alter intracellular calcium kinetics, leading to a shift in the location of calcium signal initiation sites. CGB and C-CGB were found to induce major changes in calcium kinetics, and C-CGB altered the latendy between the first somatic and neuritic calcium signals resulting in a statistical trend for shifting the calcium signal initiation site from the growth cone to the soma; whereas N-CGB diminished the interaction between $InsP_3RI$ and endogenous CGB, resulting in diminished calcium transients. It is possible that if one of these key players becomes dysregulated, the observed CGB-mediated effects could alter normal cellular function. Moreover, since the observed changes in calcium kinetics may result in cellular dysfunction, CGB could theoretically be a target for the treatment of neurological diseases, or could theoretically be altered in order to compensate for cellular responses to neurological diseases. In any case, our results also serve to reiterate how calcium as a second messenger is capable of performing a variety of functions, from neuronal outgrowth and gene transcription to apoptosis.

	Δ magnitude [AU]	duration [seconds]	response rate [percentage]	resting calcium [AU]	signal initiation [seconds]
	15 µM	*15µM*	*15µM*		$^{\Delta t}$ *[soma-neurite]* $^{(s)}$
Control	0.9 ± 0.09	99 ± 7.5	59	41 ± 1	17.2 ± 5.3
CGB	**1.8** ± 0.17***	107 ± 7.8	80	36 ± 0.9	**2.6** ± 2.2*
C-CGB	**1.8** ± 0.10***	**167** ± 12.1***	86	38 ± 0.7	**- 1** ± 2.1*
N-CGB	**0.4** ± 0.05*	125 ± 17.4	51	43 ± 0.7	

Table 03. ***Effects of CGB and CGB fragment expression in neuronally differentiated SHSY5Y cells.***

Human neuroblastoma SHSY5Y cells were transfected with CGB or CGB fragments as described in the Materials and Methods section (or see figure 1A), and neuronally differentiated for at least 8 days by incubation with retinoic acid and recombinant human nerve growth factor. Calcium imaging experiments were conducted on a Zeiss NLO confocal microscope, by loading cells with a calcium-sensitive imaging dye, fluo-4 AM. Expression of CGB or CGB-fragments were confirmed by co-transfecting cells with at least 3-fold less fluorescent DsRed2 protein. Cells were stimulated with 15 µM carbachol, an mAChR agonist, and calcium signal initiation sites and calcium kinetics were monitored. Results for peak calcium release, duration of the calcium response, response rate, total calcium release, resting calcium and the signal initiation sites are shown in the corresponding columns. Stated

*values are the result of at least 4 different and independent experiments per treatment group. Statistically significant values are shown in bold and stated as follows: * ≤ 0.01, ** ≤ 0.001, *** ≤ 0.0001.*

6.5 Effects of the expression of CGB and CGB fragments on secretory granule biogenesis

As previously mentioned, CGB was shown to induce secretory vesicle biogenesis. However, experiments conducted in CGB knock-out mice have called into question the *in vitro* secretory vesicle biogenesis results for CGA and CGB, leading to a controversy surrounding the role and importance of CGA and CGB for this process *in vivo* (Obermuller et al. 2010).

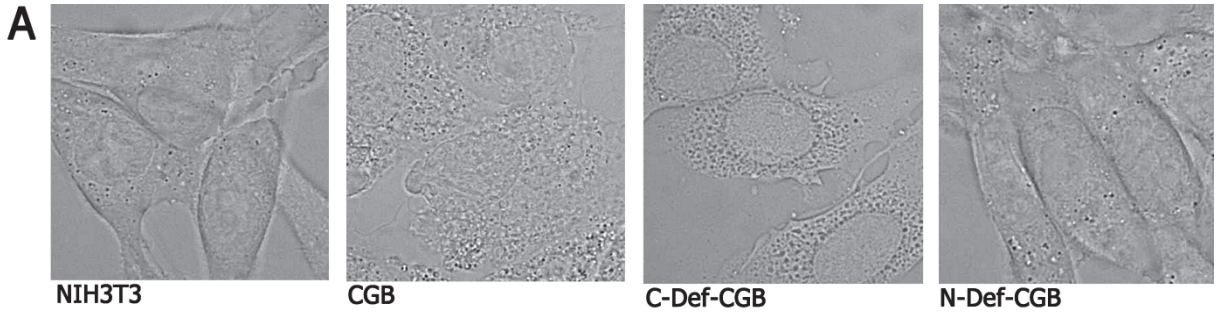

Fig. 07. ***Expression of CGB and C-Def-CGB induces de novo secretory granule biogenesis.***

Images of CGB, C-Def CGB and N-Def-CGB expressing NIH3T3 cells were recorded at 100x using a light microscope. Only C-Def-CGB and CGB expression induced de novo secretory vesicle biogenesis.

In our experiments, the region of CGB critical for secretory vesicle biogenesis was found to be located in the N-terminal region. As observed by light microscopy, control wild type NIH3T3 cells showed no indication of cytoplasmic secretory vesicle formation. However, as shown previously, expression of CGB resulted in a significant increase the number of cytoplasmic secretory vesicles. The same effect was observed following C-Def-CGB expression, in which the C-terminal region of CGB was deleted; therefore, no calcium kinetics modifying effects could be assumed. Thus, interestingly, secretory vesicle biogenesis does not seem to require the changes in calcium kinetics associated with CGB expression. Consistently, expression of N-Def-CGB led to no microscopically observable secretory vesicles. Taken together, these results indicate that the N-terminal domain of CGB is essential for secretory vesicle biogenesis. To further quantify the level of *de novo* secretory vesicle biogenesis mediated by CGB, we transfected NIH3T3 cells with CGB, C-Def-CGB, N-Def-CGB, N-CGB or C-SP (for control purposes). After expression, we

visualized CGB (or the transfected CGB fragments) and beta-COP as a secretory vesicle marker. Expression of CGB, C-Def-CGB or N-CGB in NIH3T3 cells resulted in *de novo* secretory vesicle biogenesis, whereas N-Def-CGB and C-SP did not induce secretory vesicle formation. Based on these results, fragments of CGB containing the N-terminal binding region, or even just the N-terminal region of CGB, appear to be sufficient for inducing *de novo* secretory vesicle biogenesis (figure 07, figure 08).

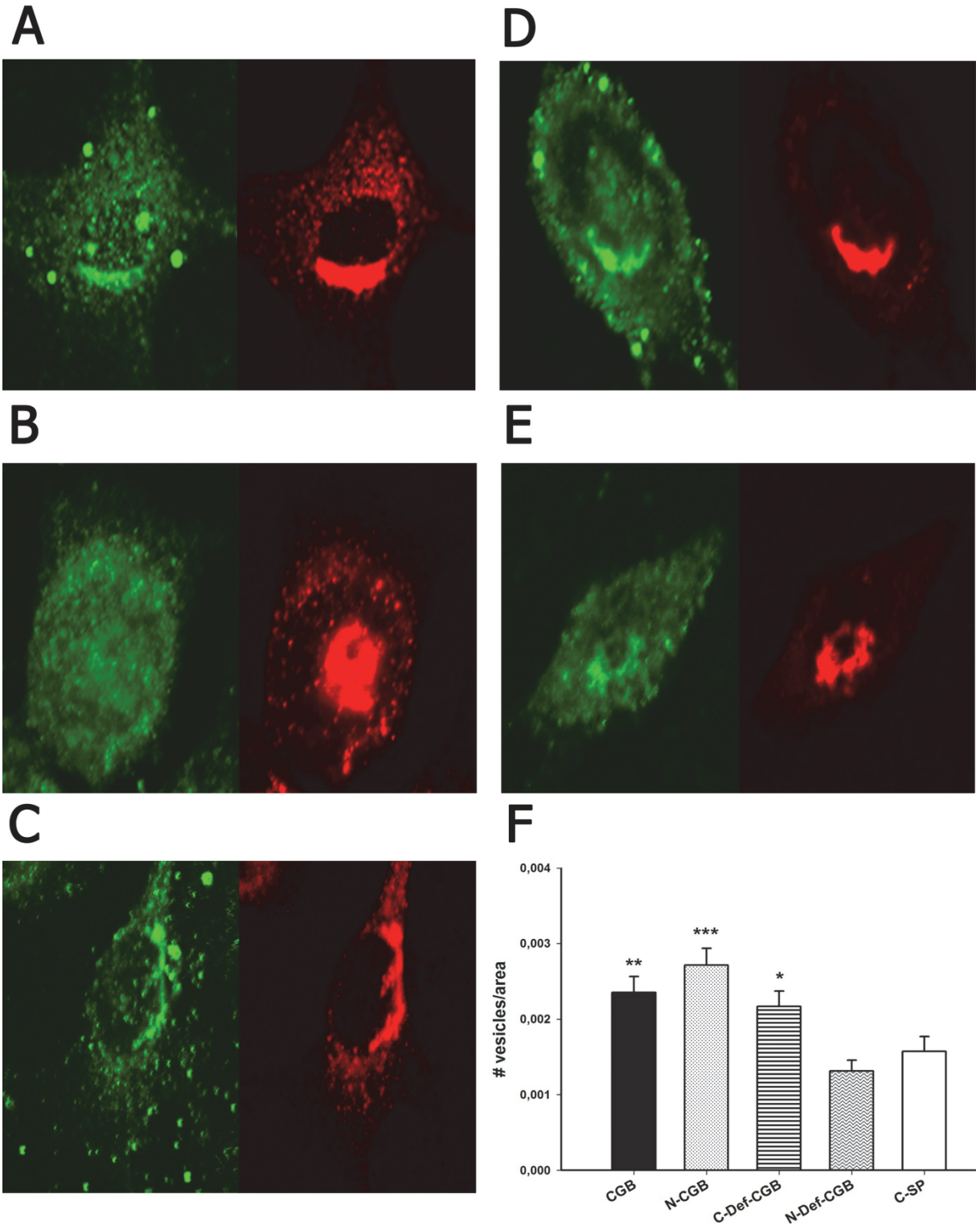

Fig. 08. ***N-CGB is required for secretory vesicle biogenesis.***

CGB fragments were expressed in NIH3T3 cells and stained for CGB or c-myc (green), and secretory vesicles (beta-COP, red). ***(A)*** *CGB,* ***(B)*** *N-CGB,* ***(C)*** *C-Def-CGB,* ***(D)*** *N-Def-CGB,* ***(E)*** *C-SP (scrambled C-CGB).* ***(F)*** *After secretory vesicle quantification, N-CGB, CGB, C-Def-CGB were found to induce vesicle biogenesis. N-Def-CGB did not increase secretory vesicle*

*biogenesis over control cells (C-SP). Data are mean ± SEM; * = p value of ≤ 0.05, ** = p value of ≤ 0.03, *** = p value of ≤ 0.01.*

Our results partly address the above mentioned controversy, since the conserved N-terminal of CGB shares a high-level of amino acid sequence similarity with CGA, and has been shown to be sufficient for induction of secretory vesicle biogenesis. When either CGA or CGB is knocked out, upregulation of the other chromogranin rescues secretory vesicle biogenesis, partly compensating for the loss of the other chromogranin. In fact, even minimal concentrations of the common N-terminal domain appear to be sufficient to induce secretory vesicle biogenesis.

6.6 Regulation of CGB in an autoimmune encephalomyelitis (EAE) mouse model for multiple sclerosis and summarized results

As outlined above, CGB is dysregulated in many neurological diseases, and is thus presumably involved in offsetting or adjusting the pathophysiological changes associated with a particular disease. Although most major neurological disease states have been found to be associated with CGB dysregulation, multiple sclerosis (MS) is a neurological disorder that has not yet been linked with CGB.

The available evidence in the literature only points to a peptide derived from CGB that is decreased in cerebrospinal fluid (CSF) in individuals diagnosed with MS (Mattsson et al. 2007). Although MS is characterized by various aspects, the reason why we chose MS as a study model was that, in theory, the demyelination caused by MS, and the resulting disruption of signal transduction, might be at least partially offset by increased expression of CGB, or expression of CGB in different cellular compartments. In particular, CGB might in particular aid in calcium-dependent gene transcription, neuronal outgrowth and downstream neuronal signal transduction.

In order to test our hypothesis, we used autoimmune encephalitis mice (EAE), a mouse model of MS, and looked at CGB expression in homogenates of different brain regions taken from these mice. In fact, interestingly, CGB expression was found to be upregulated in all of the brain regions examined. EAE mice are classified according to disease severity, which is scored depending on motor skills. These scores were found to be proportional to the degree of CGB upregulation in the cerebellum. Overall, CGB was measured to be upregulated 11-fold in cerebellum homogenates of mice with a disease severity score of 2 *versus* healthy control mice. Moreover, in samples collected from mice with a disease severity score of 2,5, upregulation of CGB increased 32-times; while a disease severity score of 3 was associated with a 91-fold CGB increase versus controls. In fact, the amount of CGB expressed in cerebellum homogenates was statistically significantly altered between mice with different severity scores, making it possible to use CGB levels as a *post mortem* biomarker for disease severity score. However, although CGB expression levels in the spinal cord, cerebral cortex and frontal cortex were significantly upregulated, no statistically significant correlation was found between CGB levels and disease severity groups (figure 09).

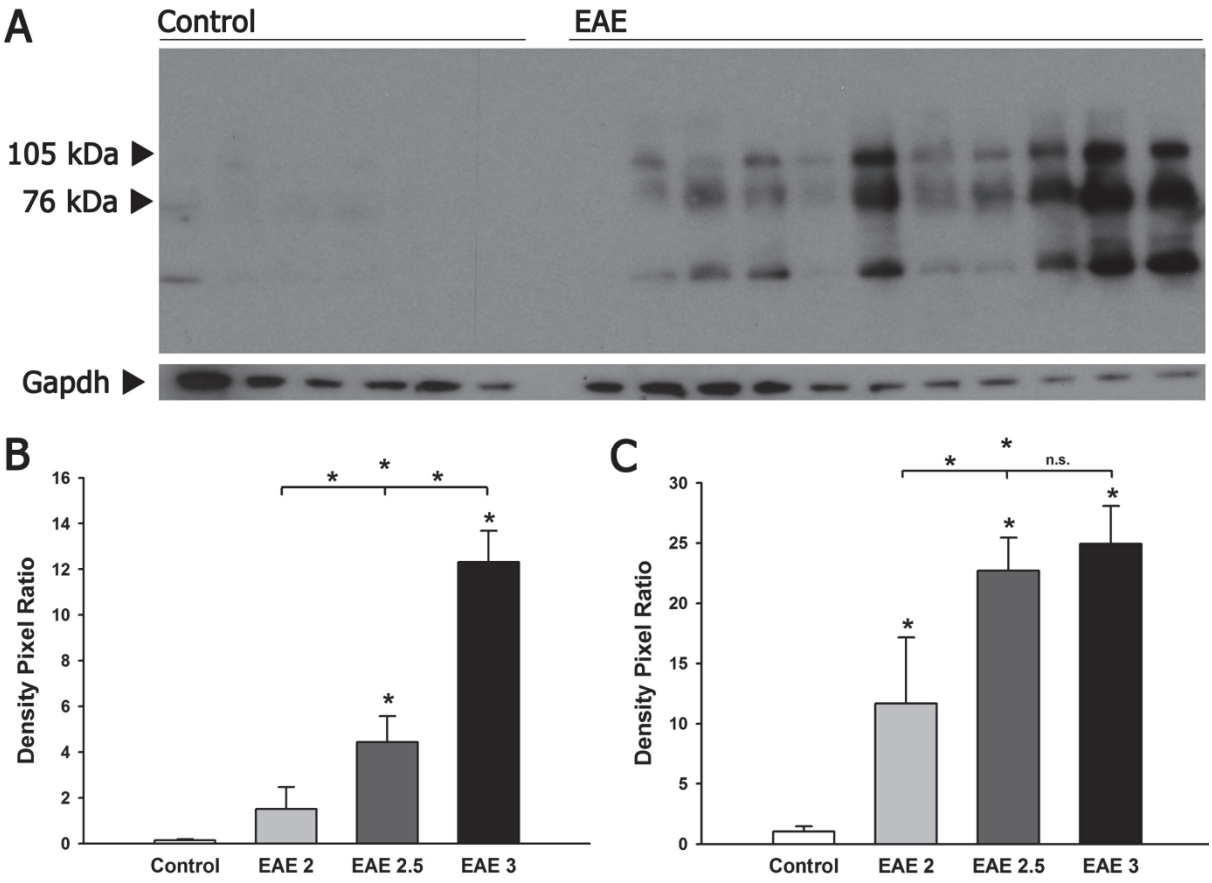

Fig. 09. ***Upregulation of CGB in different brain region homogenates in EAE mice, a mouse model for multiple sclerosis.***

Autoimmune encephalitis was induced by subcutaneous injection of myelin oligodendrocyte glycoprotein and treated mice were classified according to a disease severity score, depending on their motor skills (see Materials and Methods). Brain homogenates from the cerebellum, spinal cord, cerebral cortex and frontal cortex were obtained and used for quantitative Western blot analysis with a CGB antibody. ***(A)*** *Western blot from cerebellum homogenates of 6 healthy control mice and 11 EAE mice, Gapdh was used as a gel loading control.* ***(B)*** *Anti-CGB Western blot results from cerebellum homogenates. Very little intact CGB was detected in healthy control mice. CGB expression levels in mice with a disease severity score of 2 were upregulated 11-fold; while mice classified with a score of 2.5 showed 32-fold higher CGB expression levels; and mice with a score of 3 displayed a 92-fold increase in CGB expression. These results illustrate the functional importance of CGB in the pathogenesis of autoimmune encephalitis. Differences in CGB expression between disease severity groups were statistically significant, making it possible to use CGB expression in cerebellum homogenates as a post mortem biomarker for disease severity.* ***(C)*** *Western blot results from spinal cord homogenates. Mice classified with a disease severity score of 2 showed an 11-fold upregulation of CGB, similar to results found in the cerebellum. In mice*

classified with a score of 2.5, CGB was upregulated 21-fold; while in mice classified with a score of 3, CGB was upregulated 23-fold.

In order to test if the CGB upregulation observed in brain region homogenates is due to upregulation of CGB in neurons, and not glia cells or other neuronal cells, we used CGB stained cryosections; confirming CGB expression in the neurons (figure 10).

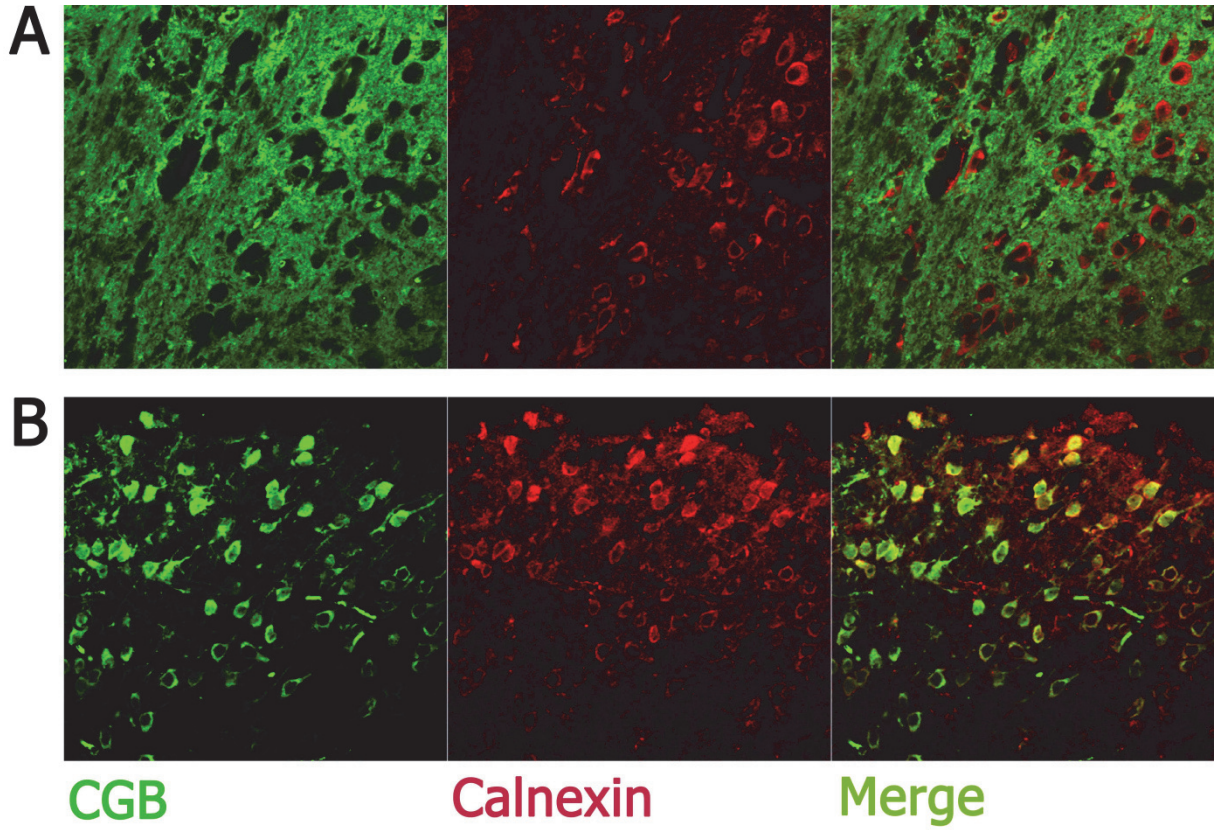

Fig. 10. ***Upregulation of CGB expression in EAE brain region homogenates is localized to neurons.***
(A) *Very little (or negligible) CGB could be detected in brain slices taken from the frontal cortex of healthy control mice. For panel 1, high amounts of anti-CGB-antibody were used, resulting in either non-specific staining, or neuritic binding of the CGB-antibody. Calnexin was used to visualize the neuronal cells in the imaged area.* ***(B)*** *In EAE mice, high levels of CGB expression was localized to the intraluminal region of the ER, as shown by the overlap with the ER marker protein calnexin. These results illustrate the functional importance of CGB in EAE pathogenesis in mice.*

In summary, CGB has been previously shown to be involved in calcium signaling, via interaction with the $InsP_3R$ at the luminal side of the ER. In addition, two potentially important regions of CGB have been identified, the N-terminal domain

and the C-terminal domain. In this thesis, we identified distinct roles for the N- and C-terminal domains of CGB, and showed their crucial importance in calcium kinetics as part of an $InsP_3RI$-CGB calcium microdomain. We further clarified the role of CGB in the maintenance and modulation of calcium signaling, as well as in secretory vesicle biogenesis.

In addition, we found that the 23aa long C-terminal domain is crucial for inducing $InsP_3R$ calcium release. Furthermore, we characterized the role of CGB and found that expression of the 20 aa long N-terminal domain is sufficient to induce *de novo* secretory vesicle biogenesis. N-CGB was also found to play a role as a competitive inhibitor of full-length CGB. When full-length CGB is present, the N-terminus competes with full-length CGB for its binding site on the $InsP_3R$, thereby decreasing calcium release. On the other hand, in cells lacking CGB, competition between full-length CGB and N-terminal CGB does not occur, resulting in unaltered calcium release.

Expression of CGB or CGB-derived fragments in neuronally differentiated PC12 or human SHSY5Y cells, was found to be associated with significantly altered signal initiation sites, illustrating the power of a calcium microdomain consisting of the $InsP_3RI$ and CGB or CGB-derived fragments.

Based on the findings presented in this thesis, we developed a hypothesis that CGB may be an important modulator in neurological disease. We attempted to test this for MS, a neurological disease where demyelination might lead to problems that could be partially offset by higher CGB expression. Consistent with this hypothesis, we found a statistically significant upregulation of CGB in brain regions of EAE mice, a mouse model for MS.

76 kDa	spinal cord	cerebellum	cerebral cortex	frontal cortex	hippocampus
Control	1.0 ± 0.4	0.1 ± 0.05	0.3 ± 0.3	0.6 ± 0.5	0.07 ± 0.04
EAE 2	**11.7** ± 5.5*	1.5 ± 1.0	1.5 ± 0.9	3.2 ± 1.6	1.5 ± 0.9
EAE 2.5	**22.7** ± 2.8***	**4.4** ± 1.1*	2.1 ± 1.1	**3.7** ± 1.0*	4.7 ± 3.0
EAE 3	**24.9** ± 3.1***	**12.3** ± 1.4***	**4.3** ± 1.1*	**7.7** ± 2.5**	1.1 ± 0.8
105 kDa	**spinal cord**	**cerebellum**	**cerebral cortex**	**frontal cortex**	**hippocampus**
Control	0.3 ± 0.1	0.07 ± 0.02	0.06 ± 0.04	0.2 ± 0.1	0.05 ± 0.01
EAE 2	**5.8** ± 2.7*	0.6 ± 0.3	0.4 ± 0.2	2.5 ± 1.0	1.0 ± 0.4
EAE 2.5	**10.5** ± 1.7***	**2.4** ± 0.8*	0.8 ± 0.4	2.7 ± 0.7	2.8 ± 2.2
EAE 3	**11.3** ± 1.9***	**5.9** ± 1.0***	**1.4** ± 0.4*	**4.3** ± 1.4**	3.1 ± 0.7

Table 04. ***Chromogranin concentrations determined by western blotting in different brain regions of EAE mice.***

*Autoimmune encephalitis was induced by subcutaneous injection of myelin oligodendrocyte glycoprotein, and affected mice were classified to a disease severity score depending on their motor skills (see Materials and Methods). Brain homogenates of the cerebellum, spinal cord, cerebral cortex, frontal cortex and hippocampus were obtained and used for quantitative Western blot analysis using an anti-CGB antibody. Note that CGB bands were detected at 76 and 105 kDa. Usually CGB runs at 76 kDa in sodium dodecyl sulfate-polyacrylamide gel electrophoresis (SDS-PAGE); however, post-translational modifications such as phosphorylation, sulforylation and glycosylation could result in a modified CGB which migrates at 105 kDa. Stated values are the result of at least 3 different and independent experiments per treatment group. Statistically significant values (vs. control group) are shown in bold and stated as follows: * ≤ 0.05, **≤ 0.01, *** ≤ 0.001.*

7. Reference List

Adkins, CE, Morris, SA, De Smedt, H, Sienaert, I, Torok, K and Taylor, CW (2000): Ca2+-calmodulin inhibits Ca2+ release mediated by type-1, -2 and -3 inositol trisphosphate receptors. Biochem J 345 Pt 2, 357-363

Allbritton, NL, Meyer, T and Stryer, L (1992): Range of messenger action of calcium ion and inositol 1,4,5-trisphosphate. Science 258, 1812-1815

Ando, H, Mizutani, A, Kiefer, H, Tsuzurugi, D, Michikawa, T and Mikoshiba, K (2006): IRBIT suppresses IP3 receptor activity by competing with IP3 for the common binding site on the IP3 receptor. Mol Cell 22, 795-806

Appell, KC and Barefoot, DS (1989): Neurotransmitter release from bradykinin-stimulated PC12 cells. Stimulation of cytosolic calcium and neurotransmitter release. Biochem J 263, 11-18

Bartolomucci, A, Pasinetti, GM and Salton, SR (2010): Granins as disease-biomarkers: translational potential for psychiatric and neurological disorders. Neuroscience 170, 289-297

Benedum, UM, Lamouroux, A, Konecki, DS, Rosa, P, Hille, A, Baeuerle, PA, Frank, R, Lottspeich, F, Mallet, J and Huttner, WB (1987): The primary structure of human secretogranin I (chromogranin B): comparison with chromogranin A reveals homologous terminal domains and a large intervening variable region. EMBO J 6, 1203-1211

Berridge, MJ (1993): Inositol trisphosphate and calcium signalling. Nature 361, 315-325

Berridge, MJ (1998): Neuronal calcium signaling. Neuron 21, 13-26

Beuret, N, Stettler, H, Renold, A, Rutishauser, J and Spiess, M (2004): Expression of regulated secretory proteins is sufficient to generate granule-like structures in constitutively secreting cells. J Biol Chem 279, 20242-20249

Bezprozvanny, I (2005): The inositol 1,4,5-trisphosphate receptors. Cell Calcium 38, 261-272

Boehning, D, Patterson, RL, Sedaghat, L, Glebova, NO, Kurosaki, T and Snyder, SH (2003): Cytochrome c binds to inositol (1,4,5) trisphosphate receptors, amplifying calcium-dependent apoptosis. Nat Cell Biol 5, 1051-1061

Bofill-Cardona, E, Vartian, N, Nanoff, C, Freissmuth, M and Boehm, S (2000): Two different signaling mechanisms involved in the excitation of rat sympathetic neurons by uridine nucleotides. Mol Pharmacol 57, 1165-1172

Bootman, MD, Collins, TJ, Peppiatt, CM, Prothero, LS, MacKenzie, L, De Smet, P, Travers, M, Tovey, SC, Seo, JT, Berridge, MJ, et al. (2001): Calcium signalling--an overview. Semin Cell Dev Biol 12, 3-10

Bourguignon, LY and Jin, H (1995): Identification of the ankyrin-binding domain of the mouse T-lymphoma cell inositol 1,4,5-trisphosphate (IP3) receptor and its role in the regulation of IP3-mediated internal Ca2+ release. J Biol Chem 270, 7257-7260

Choe, CU and Ehrlich, BE (2006): The inositol 1,4,5-trisphosphate receptor (IP3R) and its regulators: sometimes good and sometimes bad teamwork. Sci STKE 2006, re15

Choe, CU, Harrison, KD, Grant, W and Ehrlich, BE (2004): Functional coupling of chromogranin with the inositol 1,4,5-trisphosphate receptor shapes calcium signaling. J Biol Chem 279, 35551-35556

Cruzblanca, H, Koh, DS and Hille, B (1998): Bradykinin inhibits M current via phospholipase C and Ca2+ release from IP3-sensitive Ca2+ stores in rat sympathetic neurons. Proc Natl Acad Sci U S A 95, 7151-7156

Delmas, P and Brown, DA (2002): Junctional signaling microdomains: bridging the gap between the neuronal cell surface and Ca2+ stores. Neuron 36, 787-790

Delmas, P, Wanaverbecq, N, Abogadie, FC, Mistry, M and Brown, DA (2002): Signaling microdomains define the specificity of receptor-mediated InsP(3) pathways in neurons. Neuron 34, 209-220

del Rio, E, Bevilacqua, JA, Marsh, SJ, Halley, P and Caulfield, MP (1999): Muscarinic M1 receptors activate phosphoinositide turnover and Ca2+ mobilisation in rat sympathetic neurones, but this signalling pathway does not mediate M-current inhibition. J Physiol 520 Pt 1, 101-111

Eder, U, Leitner, B, Kirchmair, R, Pohl, P, Jobst, KA, Smith, AD, Mally, J, Benzer, A, Riederer, P, Reichmann, H, et al. (1998): Levels and proteolytic processing of chromogranin A and B and secretogranin II in cerebrospinal fluid in neurological diseases. J Neural Transm 105, 39-51

Erin, N and Billingsley, ML (2004): Domoic acid enhances Bcl-2-calcineurin-inositol-1,4,5-trisphosphate receptor interactions and delayed neuronal death in rat brain slices. Brain Res 1014, 45-52

Fagni, L, Worley, PF and Ango, F (2002): Homer as both a scaffold and transduction molecule. Sci STKE 2002, re8

Felder, CC (1995): Muscarinic acetylcholine receptors: signal transduction through multiple effectors. FASEB J 9, 619-625

Feng, W, Tu, J, Yang, T, Vernon, PS, Allen, PD, Worley, PF and Pessah, IN (2002): Homer regulates gain of ryanodine receptor type 1 channel complex. J Biol Chem 277, 44722-44730

Finch, EA and Augustine, GJ (1998): Local calcium signalling by inositol-1,4,5-trisphosphate in Purkinje cell dendrites. Nature 396, 753-756

Foskett, JK (2010): Inositol trisphosphate receptor Ca2+ release channels in neurological diseases. Pflugers Arch 460, 481-494

Foskett, JK, White, C, Cheung, KH and Mak, DO (2007): Inositol trisphosphate receptor Ca2+ release channels. Physiol Rev 87, 593-658

Furuichi, T, Yoshikawa, S, Miyawaki, A, Wada, K, Maeda, N and Mikoshiba, K (1989): Primary structure and functional expression of the inositol 1,4,5-trisphosphate-binding protein P400. Nature 342, 32-38

Gartner, A, Polnau, DG, Staiger, V, Sciarretta, C, Minichiello, L, Thoenen, H, Bonhoeffer, T and Korte, M (2006): Hippocampal long-term potentiation is supported by presynaptic and postsynaptic tyrosine receptor kinase B-mediated phospholipase Cgamma signaling. J Neurosci 26, 3496-3504

Gill, BM, Barbosa, JA, Dinh, TQ, Garrod, S and O'Connor, DT (1991): Chromogranin B: isolation from pheochromocytoma, N-terminal sequence, tissue distribution and secretory vesicle processing. Regul Pept 33, 223-235

Goldberg, JH, Tamas, G, Aronov, D and Yuste, R (2003): Calcium microdomains in aspiny dendrites. Neuron 40, 807-821

Gorr, SU, Shioi, J and Cohn, DV (1989): Interaction of calcium with porcine adrenal chromogranin A (secretory protein-I) and chromogranin B (secretogranin I). Am J Physiol 257, E247-254

Greene, LA and Tischler, AS (1976): Establishment of a noradrenergic clonal line of rat adrenal pheochromocytoma cells which respond to nerve growth factor. Proc Natl Acad Sci U S A 73, 2424-2428

Gros-Louis, F, Andersen, PM, Dupre, N, Urushitani, M, Dion, P, Souchon, F, D'Amour, M, Camu, W, Meininger, V, Bouchard, JP, et al. (2009): Chromogranin B P413L variant as risk factor and modifier of disease onset for amyotrophic lateral sclerosis. Proc Natl Acad Sci U S A 106, 21777-21782

Hagar, RE and Ehrlich, BE (2000): Regulation of the type III InsP(3) receptor by InsP(3) and ATP. Biophys J 79, 271-278

Hamada, K, Miyata, T, Mayanagi, K, Hirota, J and Mikoshiba, K (2002): Two-state conformational changes in inositol 1,4,5-trisphosphate receptor regulated by calcium. J Biol Chem 277, 21115-21118

Helle, KB (2004): The granin family of uniquely acidic proteins of the diffuse neuroendocrine system: comparative and functional aspects. Biol Rev Camb Philos Soc 79, 769-794

Helle, KB, Reed, RK, Ehrhart, M, Aunis, D and Hogue Angeletti, R (1990): Chromogranin A: osmotically active fragments and their susceptibility to proteolysis during lysis of the bovine chromaffin granules. Acta Physiol Scand 138, 565-574

Higo, T, Hattori, M, Nakamura, T, Natsume, T, Michikawa, T and Mikoshiba, K (2005): Subtype-specific and ER lumenal environment-dependent regulation of inositol 1,4,5-trisphosphate receptor type 1 by ERp44. Cell 120, 85-98

Hirota, J, Ando, H, Hamada, K and Mikoshiba, K (2003): Carbonic anhydrase-related protein is a novel binding protein for inositol 1,4,5-trisphosphate receptor type 1. Biochem J 372, 435-441

Huh, YH, Jeon, SH and Yoo, SH (2003): Chromogranin B-induced secretory granule biogenesis: comparison with the similar role of chromogranin A. J Biol Chem 278, 40581-40589

Huh, YH, Jeon, SH, Yoo, JA, Park, SY and Yoo, SH (2005): Effects of chromogranin expression on inositol 1,4,5-trisphosphate-induced intracellular Ca2+ mobilization. Biochemistry 44, 6122-6132

Jacob, SN, Choe, CU, Uhlen, P, DeGray, B, Yeckel, MF and Ehrlich, BE (2005): Signaling microdomains regulate inositol 1,4,5-trisphosphate-mediated intracellular calcium transients in cultured neurons. J Neurosci 25, 2853-2864

Jiang, QX, Thrower, EC, Chester, DW, Ehrlich, BE and Sigworth, FJ (2002): Three-dimensional structure of the type 1 inositol 1,4,5-trisphosphate receptor at 24 A resolution. EMBO J 21, 3575-3581

Johenning, FW, Zochowski, M, Conway, SJ, Holmes, AB, Koulen, P and Ehrlich, BE (2002): Distinct intracellular calcium transients in neurites and somata integrate neuronal signals. J Neurosci 22, 5344-5353

Joseph, SK, Boehning, D, Bokkala, S, Watkins, R and Widjaja, J (1999): Biosynthesis of inositol trisphosphate receptors: selective association with the molecular chaperone calnexin. Biochem J 342 (Pt 1), 153-161

Kang, J, Kang, S, Yoo, SH and Park, S (2007): Identification of residues participating in the interaction between an intraluminal loop of inositol 1,4,5-trisphosphate receptor and a conserved N-terminal region of chromogranin B. Biochim Biophys Acta 1774, 502-509

Kasri, NN, Holmes, AM, Bultynck, G, Parys, JB, Bootman, MD, Rietdorf, K, Missiaen, L, McDonald, F, De Smedt, H, Conway, SJ, et al. (2004): Regulation of InsP3 receptor activity by neuronal Ca2+-binding proteins. EMBO J 23, 312-321

Kato, A, Ozawa, F, Saitoh, Y, Fukazawa, Y, Sugiyama, H and Inokuchi, K (1998): Novel members of the Vesl/Homer family of PDZ proteins that bind metabotropic glutamate receptors. J Biol Chem 273, 23969-23975

Kim, T, Tao-Cheng, JH, Eiden, LE and Loh, YP (2001): Chromogranin A, an "on/off" switch controlling dense-core secretory granule biogenesis. Cell 106, 499-509

Kiselyov, K, Xu, X, Mozhayeva, G, Kuo, T, Pessah, I, Mignery, G, Zhu, X, Birnbaumer, L and Muallem, S (1998): Functional interaction between InsP3 receptors and store-operated Htrp3 channels. Nature 396, 478-482

Koizumi, S, Bootman, MD, Bobanovic, LK, Schell, MJ, Berridge, MJ and Lipp, P (1999): Characterization of elementary Ca2+ release signals in NGF-differentiated PC12 cells and hippocampal neurons. Neuron 22, 125-137

Landen, M, Grenfeldt, B, Davidsson, P, Stridsberg, M, Regland, B, Gottfries, CG and Blennow, K (1999): Reduction of chromogranin A and B but not C in the cerebrospinal fluid in subjects with schizophrenia. Eur Neuropsychopharmacol 9, 311-315

Lee, SB and Rhee, SG (1995): Significance of PIP2 hydrolysis and regulation of phospholipase C isozymes. Curr Opin Cell Biol 7, 183-189

Li, JY, Leitner, B, Lovisetti-Scamihorn, P, Winkler, H and Dahlstrom, A (1999): Proteolytic processing, axonal transport and differential distribution of chromogranins A and B, and secretogranin II (secretoneurin) in rat sciatic nerve and spinal cord. Eur J Neurosci 11, 528-544

Lovisetti-Scamihorn, P, Liang, F, Leitner, B, De Potter, W and Winkler, H (1999): Pig splenic nerve: peptides derived from chromogranins by proteolytic processing during axonal transport. Regul Pept 79, 63-67

Machado, JD, Diaz-Vera, J, Dominguez, N, Alvarez, CM, Pardo, MR and Borges, R (2010): Chromogranins A and B as regulators of vesicle cargo and exocytosis. Cell Mol Neurobiol 30, 1181-1187

Malathi, K, Li, X, Krizanova, O, Ondrias, K, Sperber, K, Ablamunits, V and Jayaraman, T (2005): Cdc2/cyclin B1 interacts with and modulates inositol 1,4,5-trisphosphate receptor (type 1) functions. J Immunol 175, 6205-6210

Marksteiner, J, Lechner, T, Kaufmann, WA, Gurka, P, Humpel, C, Nowakowski, C, Maier, H and Jellinger, KA (2000): Distribution of chromogranin B-like immunoreactivity in the human hippocampus and its changes in Alzheimer's disease. Acta Neuropathol 100, 205-212

Mattsson, N, Ruetschi, U, Podust, VN, Stridsberg, M, Li, S, Andersen, O, Haghighi, S, Blennow, K and Zetterberg, H (2007): Cerebrospinal fluid concentrations of peptides derived from chromogranin B and secretogranin II are decreased in multiple sclerosis. J Neurochem 103, 1932-1939

Mehta, D, Ahmmed, GU, Paria, BC, Holinstat, M, Voyno-Yasenetskaya, T, Tiruppathi, C, Minshall, RD and Malik, AB (2003): RhoA interaction with inositol 1,4,5-trisphosphate receptor and transient receptor potential channel-1 regulates Ca2+ entry. Role in signaling increased endothelial permeability. J Biol Chem 278, 33492-33500

Michikawa, T, Hirota, J, Kawano, S, Hiraoka, M, Yamada, M, Furuichi, T and Mikoshiba, K (1999): Calmodulin mediates calcium-dependent inactivation of the cerebellar type 1 inositol 1,4,5-trisphosphate receptor. Neuron 23, 799-808

Mikoshiba, K (2007): IP3 receptor/Ca2+ channel: from discovery to new signaling concepts. J Neurochem 102, 1426-1446

Mikoshiba, K, Furuichi, T and Miyawaki, A (1994): Structure and function of IP3 receptors. Semin Cell Biol 5, 273-281

Miyakawa, T, Maeda, A, Yamazawa, T, Hirose, K, Kurosaki, T and Iino, M (1999): Encoding of Ca2+ signals by differential expression of IP3 receptor subtypes. EMBO J 18, 1303-1308

Miyata, M, Finch, EA, Khiroug, L, Hashimoto, K, Hayasaka, S, Oda, SI, Inouye, M, Takagishi, Y, Augustine, GJ and Kano, M (2000): Local calcium release in dendritic spines required for long-term synaptic depression. Neuron 28, 233-244

Nimchinsky, EA, Sabatini, BL and Svoboda, K (2002): Structure and function of dendritic spines. Annu Rev Physiol 64, 313-353

Nowakowski, C, Kaufmann, WA, Adlassnig, C, Maier, H, Salimi, K, Jellinger, KA and Marksteiner, J (2002): Reduction of chromogranin B-like immunoreactivity in distinct subregions of the hippocampus from individuals with schizophrenia. Schizophr Res 58, 43-53

Obermuller, S, Calegari, F, King, A, Lindqvist, A, Lundquist, I, Salehi, A, Francolini, M, Rosa, P, Rorsman, P, Huttner, WB, et al. (2010): Defective secretion of islet hormones in chromogranin-B deficient mice. PLoS One 5, e8936

Patel, S, Morris, SA, Adkins, CE, O'Beirne, G and Taylor, CW (1997): Ca2+-independent inhibition of inositol trisphosphate receptors by calmodulin: redistribution of calmodulin as a possible means of regulating Ca2+ mobilization. Proc Natl Acad Sci U S A 94, 11627-11632

Patterson, RL, van Rossum, DB, Barrow, RK and Snyder, SH (2004): RACK1 binds to inositol 1,4,5-trisphosphate receptors and mediates Ca2+ release. Proc Natl Acad Sci U S A 101, 2328-2332

Patterson, RL, van Rossum, DB, Kaplin, AI, Barrow, RK and Snyder, SH (2005): Inositol 1,4,5-trisphosphate receptor/GAPDH complex augments Ca2+ release via locally derived NADH. Proc Natl Acad Sci U S A 102, 1357-1359

Phillips, JH (1982): Dynamic aspects of chromaffin granule structure. Neuroscience 7, 1595-1609

Rizzuto, R and Pozzan, T (2006): Microdomains of intracellular Ca2+: molecular determinants and functional consequences. Physiol Rev 86, 369-408

Rossier, MF, Bird, GS and Putney, JW, Jr. (1991): Subcellular distribution of the calcium-storing inositol 1,4,5-trisphosphate-sensitive organelle in rat liver. Possible linkage to the plasma membrane through the actin microfilaments. Biochem J 274 (Pt 3), 643-650

Ruetschi, U, Zetterberg, H, Podust, VN, Gottfries, J, Li, S, Hviid Simonsen, A, McGuire, J, Karlsson, M, Rymo, L, Davies, H, et al. (2005): Identification of CSF biomarkers for frontotemporal dementia using SELDI-TOF. Exp Neurol 196, 273-281

Sabatini, BL, Oertner, TG and Svoboda, K (2002): The life cycle of Ca(2+) ions in dendritic spines. Neuron 33, 439-452

Schlecker, C, Boehmerle, W, Jeromin, A, DeGray, B, Varshney, A, Sharma, Y, Szigeti-Buck, K and Ehrlich, BE (2006): Neuronal calcium sensor-1 enhancement of

InsP3 receptor activity is inhibited by therapeutic levels of lithium. J Clin Invest 116, 1668-1674

Schmidt, H, Stiefel, KM, Racay, P, Schwaller, B and Eilers, J (2003): Mutational analysis of dendritic Ca2+ kinetics in rodent Purkinje cells: role of parvalbumin and calbindin D28k. J Physiol 551, 13-32

Schrott-Fischer, A, Bitsche, M, Humpel, C, Walcher, C, Maier, H, Jellinger, K, Rabl, W, Glueckert, R and Marksteiner, J (2009): Chromogranin peptides in amyotrophic lateral sclerosis. Regul Pept 152, 13-21

Shafer, TJ and Atchison, WD (1991): Transmitter, ion channel and receptor properties of pheochromocytoma (PC12) cells: a model for neurotoxicological studies. Neurotoxicology 12, 473-492

Soler-Llavina, GJ and Sabatini, BL (2006): Synapse-specific plasticity and compartmentalized signaling in cerebellar stellate cells. Nat Neurosci 9, 798-806

Sugiyama, T, Matsuda, Y and Mikoshiba, K (2000): Inositol 1,4,5-trisphosphate receptor associated with focal contact cytoskeletal proteins. FEBS Lett 466, 29-34

Taufiq, AM, Fujii, S, Yamazaki, Y, Sasaki, H, Kaneko, K, Li, J, Kato, H and Mikoshiba, K (2005): Involvement of IP3 receptors in LTP and LTD induction in guinea pig hippocampal CA1 neurons. Learn Mem 12, 594-600

Taupenot, L, Harper, KL and O'Connor, DT (2003): The chromogranin-secretogranin family. N Engl J Med 348, 1134-1149

Thrower, EC, Park, HY, So, SH, Yoo, SH and Ehrlich, BE (2002): Activation of the inositol 1,4,5-trisphosphate receptor by the calcium storage protein chromogranin A. J Biol Chem 277, 15801-15806

Thrower, EC, Choe, CU, So, SH, Jeon, SH, Ehrlich, BE and Yoo, SH (2003): A functional interaction between chromogranin B and the inositol 1,4,5-trisphosphate receptor/Ca2+ channel. J Biol Chem 278, 49699-49706

Treves, S, Franzini-Armstrong, C, Moccagatta, L, Arnoult, C, Grasso, C, Schrum, A, Ducreux, S, Zhu, MX, Mikoshiba, K, Girard, T, et al. (2004): Junctate is a key element in calcium entry induced by activation of InsP3 receptors and/or calcium store depletion. J Cell Biol 166, 537-548

Tu, JC, Xiao, B, Yuan, JP, Lanahan, AA, Leoffert, K, Li, M, Linden, DJ and Worley, PF (1998): Homer binds a novel proline-rich motif and links group 1 metabotropic glutamate receptors with IP3 receptors. Neuron 21, 717-726

Tu, JC, Xiao, B, Naisbitt, S, Yuan, JP, Petralia, RS, Brakeman, P, Doan, A, Aakalu, VK, Lanahan, AA, Sheng, M, et al. (1999): Coupling of mGluR/Homer and PSD-95 complexes by the Shank family of postsynaptic density proteins. Neuron 23, 583-592

Urushitani, M, Sik, A, Sakurai, T, Nukina, N, Takahashi, R and Julien, JP (2006): Chromogranin-mediated secretion of mutant superoxide dismutase proteins linked to amyotrophic lateral sclerosis. Nat Neurosci 9, 108-118

Vanderheyden, V, Devogelaere, B, Missiaen, L, De Smedt, H, Bultynck, G and Parys, JB (2009): Regulation of inositol 1,4,5-trisphosphate-induced Ca2+ release by reversible phosphorylation and dephosphorylation. Biochim Biophys Acta 1793, 959-970

van Rossum, DB, Patterson, RL, Cheung, KH, Barrow, RK, Syrovatkina, V, Gessell, GS, Burkholder, SG, Watkins, DN, Foskett, JK and Snyder, SH (2006): DANGER, a novel regulatory protein of inositol 1,4,5-trisphosphate-receptor activity. J Biol Chem 281, 37111-37116

Walker, DS, Ly, S, Lockwood, KC and Baylis, HA (2002): A direct interaction between IP(3) receptors and myosin II regulates IP(3) signaling in C. elegans. Curr Biol 12, 951-956

White, C, Yang, J, Monteiro, MJ and Foskett, JK (2006): CIB1, a ubiquitously expressed Ca2+-binding protein ligand of the InsP3 receptor Ca2+ release channel. J Biol Chem 281, 20825-20833

Winkler, H and Westhead, E (1980): The molecular organization of adrenal chromaffin granules. Neuroscience 5, 1803-1823

Worley, PF, Zeng, W, Huang, G, Kim, JY, Shin, DM, Kim, MS, Yuan, JP, Kiselyov, K and Muallem, S (2007): Homer proteins in Ca2+ signaling by excitable and non-excitable cells. Cell Calcium 42, 363-371

Xiao, B, Tu, JC and Worley, PF (2000): Homer: a link between neural activity and glutamate receptor function. Curr Opin Neurobiol 10, 370-374

Yasuhara, O, Kawamata, T, Aimi, Y, McGeer, EG and McGeer, PL (1994): Expression of chromogranin A in lesions in the central nervous system from patients with neurological diseases. Neurosci Lett 170, 13-16

Yoo, SH (2010): Secretory granules in inositol 1,4,5-trisphosphate-dependent Ca2+ signaling in the cytoplasm of neuroendocrine cells. FASEB J 24, 653-664

Yoo, SH, You, SH, Kang, MK, Huh, YH, Lee, CS and Shim, CS (2002): Localization of the secretory granule marker protein chromogranin B in the nucleus. Potential role in transcription control. J Biol Chem 277, 16011-16021

Yoshioka, M, Yamazaki, Y, Fujii, S, Kaneko, K, Kato, H and Mikoshiba, K (2010): Intracellular calcium ion dynamics involved in long-term potentiation in hippocampal CA1 neurons in mice lacking the IP3 type 1 receptor. Neurosci Res 67, 149-155

Yuan, Z, Cai, T, Tian, J, Ivanov, AV, Giovannucci, DR and Xie, Z (2005): Na/K-ATPase tethers phospholipase C and IP3 receptor into a calcium-regulatory complex. Mol Biol Cell 16, 4034-4045

Zhang, B, Tan, Z, Zhang, C, Shi, Y, Lin, Z, Gu, N, Feng, G and He, L (2002): Polymorphisms of chromogranin B gene associated with schizophrenia in Chinese Han population. Neurosci Lett 323, 229-233

Zhang, S, Mizutani, A, Hisatsune, C, Higo, T, Bannai, H, Nakayama, T, Hattori, M and Mikoshiba, K (2003): Protein 4.1N is required for translocation of inositol 1,4,5-

trisphosphate receptor type 1 to the basolateral membrane domain in polarized Madin-Darby canine kidney cells. J Biol Chem 278, 4048-4056

Inhalt

1. Table of Contents I

2. List of Abbreviations..... III

8. Publications

1.)

C-terminal domain of chromogranin B regulates intracellular calcium signaling as published on October 19th 2011 in the Journal of Biological Chemistry

http://www.ncbi.nlm.nih.gov/pubmed/22016391

http://www.jbc.org/content/286/52/44888.long

2.)

The role of chromogranin B in an animal model of multiple sclerosis as published on April 24th in the Journal of Molecular and Cellular Neuroscience

http://www.ncbi.nlm.nih.gov/pubmed/23624073

http://www.sciencedirect.com/science/article/pii/S1044743113000511